

Review

# Ethylene Oligomerization Catalyzed by Different Homogeneous or Heterogeneous Catalysts

Anfeng Peng <sup>†</sup>, Zheng Huang <sup>†</sup> and Gang Li <sup>\*†</sup> 

State Key Laboratory of Fine Chemicals, School of Chemical Engineering, Dalian University of Technology, Dalian 116024, China; pengaf@mail.dlut.edu.cn (A.P.); hz22245199@mail.dlut.edu.cn (Z.H.)

\* Correspondence: liganghg@dlut.edu.cn

<sup>†</sup> These authors contributed equally to this work.

**Abstract:** Linear  $\alpha$ -olefins (LAOs) are linear alkenes with double bonds at the ends of the molecular chains. LAOs with different chain lengths can be widely applied in various fields. Ethylene oligomerization has become the main process for producing LAOs. In this review, different homogeneous or heterogeneous catalysts recently reported in ethylene oligomerization with Ni, Fe, Co, Cr, etc., as active centers will be discussed. In the homogeneous catalytic system, we mainly discuss the effects of the molecular structure and the electronic and coordination states of complexes on their catalytic activity and selectivity. The Ni, Fe, and Co homogeneous catalysts are discussed separately based on different ligand types, while the Cr-based homogeneous catalysts are discussed separately for ethylene trimerization, tetramerization, and non-selective oligomerization. In heterogeneous catalytic systems, we mainly concentrate on the influence of various supports (metal–organic frameworks, covalent organic frameworks, molecular sieves, etc.) and different ways to introduce active centers to affect the performance in ethylene oligomerization. Finally, a summary and outlook on ethylene oligomerization catalysts are provided based on the current research. The development of highly selective  $\alpha$ -olefin formation processes remains a major challenge for academia and industry.

**Keywords:** ethylene oligomerization; linear  $\alpha$ -olefins; homogeneous catalysts; heterogeneous catalysts; Ni; Fe; Co; Cr



**Citation:** Peng, A.; Huang, Z.; Li, G. Ethylene Oligomerization Catalyzed by Different Homogeneous or Heterogeneous Catalysts. *Catalysts* **2024**, *14*, 268. <https://doi.org/10.3390/catal14040268>

Academic Editors: Narendra Kumar, Leonarda Liotta and Konstantin Ivanov Hadjiivanov

Received: 27 March 2024

Revised: 13 April 2024

Accepted: 13 April 2024

Published: 17 April 2024



**Copyright:** © 2024 by the authors. Licensee MDPI, Basel, Switzerland. This article is an open access article distributed under the terms and conditions of the Creative Commons Attribution (CC BY) license (<https://creativecommons.org/licenses/by/4.0/>).

## 1. Introduction

Linear  $\alpha$ -olefins (LAOs) are linear alkenes with double bonds at the ends of the molecular chains. Due to their unique structure, they are applied widely in various fields depending on the chain length. For example, 1-butene and 1-octene are often used as copolymerization monomers for linear low-density polyethylene (LLDPE) and polyolefin elastomers (POE) [1]. LAOs with carbon numbers of 6–30 are used as important raw materials for the synthesis of plasticizers, detergents, surfactants, and other chemical products. LAOs have developed extremely rapidly in recent years, with the demand growing year after year around the world [2]. Most of the currently commercialized LAO units mainly produce full-fraction  $\alpha$ -olefins, which can meet a variety of downstream markets, with product carbon number distributions ranging from  $C_4$  to  $C_{30}^+$ . However, owing to the different demand in markets for various fractions of LAO products, the technology of producing linear  $\alpha$ -olefins with specific carbon numbers has also received attention.

Compared with wax pyrolysis [3], Fischer–Tropsch synthesis [4–6], and alkane dehydrogenation [7–9], the ethylene oligomerization method has become the main process for producing LAOs due to its relatively mild operating conditions, flexible product distribution, and high linearity. According to literature reports, there are a wide variety of catalysts for ethylene oligomerization, mainly Ni, Fe, Co, and Cr as metal active centers [10–13], and some catalysts have been industrialized to produce linearity  $\alpha$ -olefin products. For example, the Shell higher olefin process (SHOP) is an important catalytic system for ethylene

oligomerization, with more than one million tons of  $\alpha$ -olefins prepared industrially via this method [14]. Chevron Phillips realized the industrial production of 1-hexene using a Cr catalyst in 2003 [15].

The mechanism of ethylene oligomerization can be divided into the Cossee–Arlman mechanism and the metallacyclic mechanism. As early as 1966, Cossee [16] proposed the mechanism of cis-ligand insertion. After the enrichment by Arlman [17], the Cossee–Arlman mechanism (Figure 1) successfully demonstrated the process of catalyzing ethylene oligomerization to  $\alpha$ -olefins. The mechanism is divided into four steps: (i) coordination between ethylene monomer and metal active centers; (ii) ethylene insertion into metal hydride or alkyl intermediate; (iii) repeated coordination and insertion to promote chain growth; and (iv)  $\beta$ -H elimination reaction to obtain  $\alpha$ -olefins and regain active centers. The products obtained from the catalytic process following the Cossee–Arlman mechanism tend to follow a Schulz–Flory or Poisson distribution, with a wide distribution range and no specific carbon number.

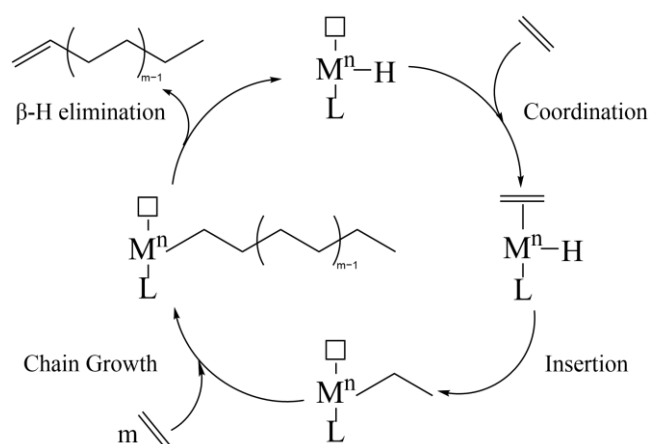


**Figure 1.** Cossee–Arlman mechanism.

However, Cr-based catalysts can produce 1-hexene and 1-octene through the catalytic tri/tetramerization of ethylene, which cannot be explained by the Cossee–Arlman mechanism. In 1989, Briggs [18] optimized the 2-ethylhexanoate chromium system and validated the metallacyclic mechanism (as shown in Figure 2) to explain the trimerization phenomenon. Chhabra et al. [19] used kinetics and deuterium isotope labeling techniques to identify intermediate species in the catalytic process of chromium diethylene complexes, further validating the metallacyclic mechanism. The mechanism for ethylene trimerization is divided into four steps: (i) two ethylene molecules coordinate with Cr; (ii) oxidative coupling to generate metallacyclopentane intermediates; (iii) insert another ethylene molecule to form a metalcycloheptane intermediate; and (iv) H-shift or  $\beta$ -H elimination and reductive elimination to generate 1-hexene. In the process of ethylene tetramerization, the third step of the metal ring mechanism is the insertion of two ethylene molecules into the metallacyclopentane intermediate to form a metalcyclononane intermediate.

This review will discuss the different homogeneous or heterogeneous catalysts reported in ethylene oligomerization with Ni, Fe, Co, and Cr as active centers. Homogeneous catalysts of various metals exhibit high activity, good selectivity, mild reaction conditions, and ligand modifiability in ethylene oligomerization, while heterogeneous catalysts have the characteristics of easy product separation and good thermal stability. In this review, the Ni, Fe, and Co homogeneous catalysts are discussed separately based on different ligand types, while the Cr-based homogeneous catalysts are discussed separately for ethylene trimerization, tetramerization, and non-selective oligomerization. Meanwhile, the Ni, Fe, Co, and Cr heterogeneous catalysts with different supports are discussed. In addition, zinc-, ruthenium-, and gallium-based heterogeneous catalysts are also mentioned. Finally, a summary and outlook on ethylene oligomerization catalysts are provided based on the current research.

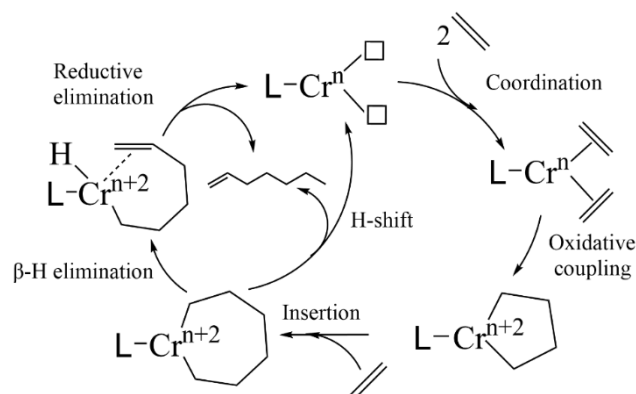


Figure 2. Metallacyclic mechanism.

## 2. Nickel-Based Catalysts

### 2.1. Nickel-Based Homogeneous Catalysts

In the 1950s, researchers discovered the “nickel effect” [20], in which ethylene and triethylaluminium were induced to form butenes in the presence of small amounts of nickel salts. The discovery stimulated the investigation of post-transition-metal-catalyzed ethylene oligomerization. In 1966, the concept of “ligand” was introduced, which further improved the development of transition metal catalysts. Shortly thereafter, Keim [21] designed neutral (P, O) ligands for ethylene oligomerization to produce linear  $\alpha$ -olefins. In 1990, Keim invented the typical SHOP catalyst (Figure 3), which became a remarkable milestone for the oligomerization reaction in industry. Another important breakthrough was the development of a highly electrophilic cationic nickel complex bearing  $\alpha$ -diimine ligands by Brookhart [22] and co-workers in 1995 (Figure 4). When the substituent in the neighboring position of the benzene ring is small (e.g., H), the polymerization of ethylene produces a low-molecular-weight oligomerization product; when the substituent resistance is gradually increased ( $\text{CH}_3$  to  $i\text{Pr}$ ), the molecular weight of the polyethylene increases as well. This finding suggests that the selectivity can be altered by changing the site resistance of the ligand in nickel complexes. Following this breakthrough, the influence of electronic effects on catalytic performance was investigated by Tuskaev et al. [23,24]. Further investigations of nickel complexes bearing  $\alpha$ -diimine ligands have involved the modification of the ligand to alter its spatial site resistance and electronic effects.

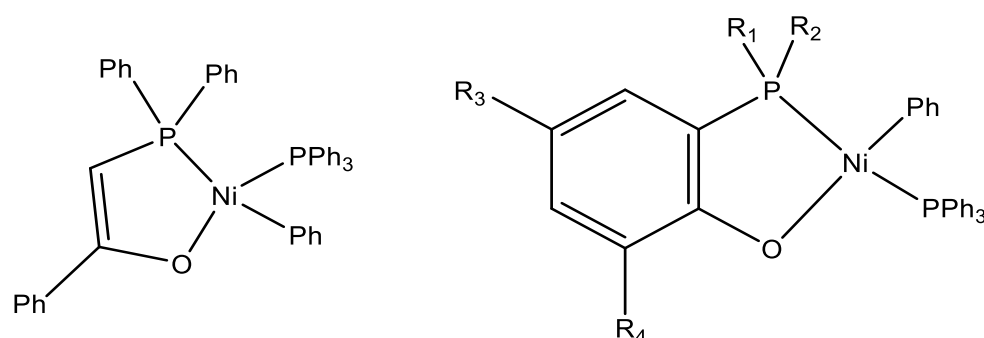
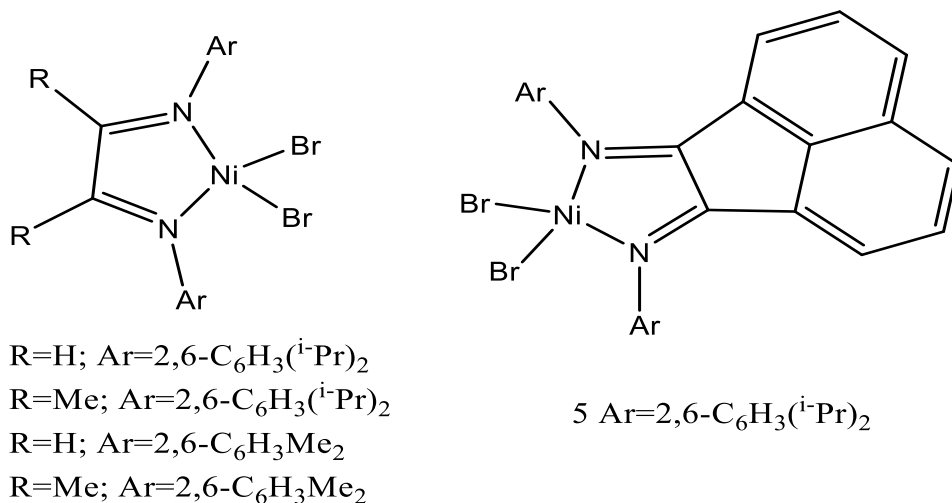


Figure 3. Nickel complex bearing neutral (P, O) ligands.

In addition, other types of bidentate ligands (including (N, O) [25–29], (P, N) [30–32], (P, P) [33–35], (P, S) [36], and (N, S) [37]) as well as tridentate ligands (including (N, N, N) [38–40], (N, N, O) [41,42], (N, O, O) [43,44], etc.) were synthesized. These above ligands have been discussed in detail by Giyjaz E. Bektukhamedov [45] and H. Olivier-Bourbigou [46] and will not be repeated here. The nickel complexes with tridentate ligands have better selectivity for linear  $\alpha$ -olefins than the didentate nickel complexes, but the activity is lower. On the whole, the bidentate ligands are still a hotspot of the current

research. The main thrust of the research has been to modify the selectivity and activity by changing the structure of the ligand in the catalyst.



**Figure 4.** Nickel complex bearing  $\alpha$ -diimine ligands.

## 2.2. Nickel-Based Heterogeneous Catalysts

Compared with homogeneous catalysts, heterogeneous catalysts have the advantages of easy separation, convenient recovery, and high selectivity. Heterogeneous catalysts have the ability to tailor the synthesized product with controlled chain length and distribution. The use of heterogeneous molecular species allows the active sites to be separated from each other, thus preventing them from aggregating or interacting, which may lead to catalyst deactivation or undesired reactivity [47]. The currently available heterogeneous catalysts for the oligomerization of ethylene include metal–organic frameworks (MOFs), covalent organic frameworks (COFs), molecular sieve materials, and other materials.

### 2.2.1. Metal–Organic Frameworks (MOFs)

Metal–organic frameworks (MOFs), known as crystalline porous coordination polymers, are crystalline solids assembled by linking metal ions or clusters with ligand molecules [48]. In recent years, MOFs have demonstrated promise as catalysts for olefin oligomerization and polymerization. MOFs possess numerous active sites separated from each other, which offers opportunities for sufficient coordination between the active center and monomer. MOFs not only have unsaturated metal sites themselves (self-assembly) but can also introduce active metal sites through post-synthetic modifications (cation exchange, atomic deposition, or ligand metalation) (Figure 5). In this section, a comprehensive contrast of MOFs for olefin oligomerization in past decades is summarized (Table 1). The highest activity of each catalyst as well as the reaction conditions (including temperature, pressure, and solvent) and selectivity for the product under the highest activity (For calculations of activity, please see Appendix A) were listed. It can be seen from Table 1 that the nickel-based heterogeneous catalysts are dominated by ethylene dimerization, regardless of the method of introducing the nickel active site and structure of the MOFs [49]. One reason may be that the lack of a large steric hindrance group around the nickel active site in the microenvironment of Ni-based MOFs leads to fast  $\beta$ -H elimination [50,51]. Another reason could be the higher nuclear charge number of nickel metals in the microenvironment, which facilitates  $\beta$ -H elimination to produce dimers [52]. As can be seen in Table 1, the current catalyst with the highest ethylene dimerization activity is Ni-ZIF-8 (0.4 wt%), synthesized using the self-assembly method reported by Chen's group [53], and the selectivity of 1-butene can be maintained above 80%. The most promising nickel-based MOFs material capable of catalyzing the trimerization of ethylene is MIL-125(Ti)-NH<sub>2</sub>(Ni), obtained by Wang et al. [54]. In the presence of the MAO co-catalyst, the total selectivity to 1-hexene can reach about 80% while achieving the highest activity.

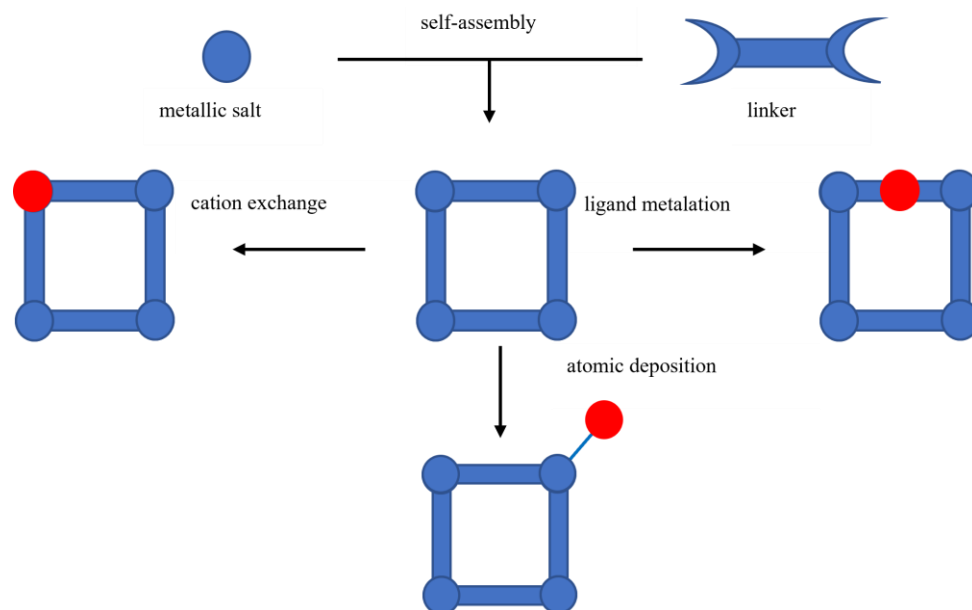


**Figure 5.** Different synthetic pathways to obtain isolated active sites within MOFs.

All the above-mentioned catalysts in the presence of alkylaluminium co-catalysts form nickel active centers, which undergo coordination insertion with ethylene and  $\beta$ -H elimination to produce linear  $\alpha$ -olefins. Moreover, some Ni-MOF materials can directly catalyze ethylene oligomerization without co-catalysts. Bhan [55] and co-workers reported Ni-functionalized UiO-66 via the atomic deposition technique. Ni/UiO-66 that uniquely engenders active sites on stream maintains stable oligomerization rates for over 15 days under gas-phase conditions without any external co-catalyst. The authors demonstrated that the number of active sites involved in the reaction indeed increases with increasing ethylene pressures using in situ NO titration. Steady-state oligomerization kinetics are proposed to follow the Cossee–Arman mechanism by comparing experimental and computed apparent activation enthalpies. Olsbye [56] and co-workers synthesized a series of UiO-67-bpy MOFs with biphenyl-4,4'-dicarboxylate (bpdc) and different amounts of 2,2'-bipyridine-5,5'-dicarboxylate (bpydc). The post-synthetic metalation of the MOFs was carried out in EtOH with Ni(acetate) $_2$ ·4H $_2$ O as the metal source. Ni-UiO-67-bpy $_{11\%}$  can catalyze the dimerization of flowing ethene (P(ethene) = 26 bar, 250 °C, Time = 240 min) with an activity up to 850 mg butene g $_{cat}^{-1}$ h $^{-1}$  after activation at 300 °C in 10% O $_2$  for 360 min. This catalyst achieves 6% conversion and 99% selectivity for linear butene (1-butene:trans-2-butene:cis-2-butene ratio was 41:26:32), which is attributed to homogeneously distributed active sites in the microenvironment and spatial confinement.

### 2.2.2. Covalent Organic Frameworks (COFs)

Covalent organic frameworks are a class of organic porous crystalline materials linked with light elements (such as H, B, C, N, O, etc.) by robust covalent bonds via reticular chemistry [57]. COFs have promising applications in the field of heterogeneous catalysis due to their ability to induce catalytically relevant ligands into their structure. Unlike conventional support materials (zeolite, metal oxide, etc.), COFs are structurally predesignable, synthetically controllable, and functionally manageable, suggesting that COFs may be another promising support material for olefin oligomerization analogues to MOFs. Since COFs have no active metal sites, they need to be modified by ligand metallization methods. Gascon et al. [58] synthesized Covalent Triazine Frameworks (CTFs) with micro- and mesoporous structures and a lamellar-structured imine-linked polymer network (IL-PON). The materials were metalated afterwards with nickel(II) bromide ethylene glycol dimethyl ether salt (NiBr $_2$ ·DME) in THF to afford the three catalysts Ni@meso-CTF, Ni@microCTF, and Ni@IL-PON. Ni can either be chemically coordinated to the nitrogen functional sites

of the backbone or remain on the surface and in the pores as uncoordinated complexes. Ni@meso-CTF, Ni@microCTF, and Ni@IL-PON, respectively, achieved an intrinsic catalytic activity of 75.3, 63, and 92.5 mol<sub>ethylene converted</sub> mol<sup>-1</sup><sub>Ni</sub> h<sup>-1</sup>, with respective butene selectivity of 59%, 54%, and 58% in the conditions of 50 °C, 15 bar of ethylene, heptane solvent, and Et<sub>3</sub>Al cocatalyst.

Li et al. [59] reported two covalent organic frameworks (COFs), MABD-COF and MAPA-COF, used in ethylene oligomerization. The specific surface area and the pore volume of MAPA-COF with p-phthalaldehyde as a sub-constructing unit were far larger than those of MABD-COF with butanedione as a sub-constructing unit. Ni@MAPA-COF and Ni@MABD-COF were obtained by metallization with nickel dichloride. The Ni-loaded COFs were evaluated for ethylene oligomerization using MAO as a cocatalyst (Al/Ni = 500 to 700), and the best activity was found in toluene as a solvent at 25 °C with a productivity of  $8.31 \times 10^4$  g mol<sup>-1</sup><sub>Ni</sub> h<sup>-1</sup> and 1-butene selectivity of 59% using Ni@MABD-COF and a productivity of  $15.68 \times 10^4$  g mol<sup>-1</sup><sub>Ni</sub> h<sup>-1</sup> and 1-butene selectivity of 51% using Ni@MAPA-COF. Recently, another group [60] reported another nickel-coordinated imine-linked covalent organic frameworks material (COF-PD-Ni) for ethylene oligomerization with a productivity of  $1.98 \times 10^5$  g mol<sup>-1</sup><sub>Ni</sub> h<sup>-1</sup>. In the condition with the highest activity, the selectivity of the product C<sub>4</sub> can reach 82%, and the remaining product is C<sub>6</sub>–C<sub>10</sub>.

### 2.2.3. Molecular Sieve Materials

Molecular sieves, as a kind of important catalyst carrier, are different from MOFs and COFs. Not only can they introduce active metal sites by ion-exchange or graft modification but they also have their own Brønsted acid sites. Acid sites are responsible not only for isomerization reactions but also for the dimerization of the primary products. Molecular sieve catalysts are able to catalyze ethylene oligomerization at high temperatures without the need for other cocatalysts to initiate the reaction. The activity (ethylene conversion) of these heterogeneous catalysts is determined by the number of accessible nickel sites, whereas the stability of the oligomerization, the carbon number distribution, and the structure of the product are determined by the concentration of Brønsted acid sites and the porosity.

Hulea et al. [61] synthesized the nickel ion-exchanged NiMCM-22 (Si/Al = 14) and NiMCM-36 (Si/Al = 26) for ethylene oligomerization reactions. The NiMCM-36 catalyst with a large mesoporous structure and mild acidity showed good activity (46 g/(g<sub>cat</sub>·h) of oligomer) and selectivity (100% of olefins with an even number of carbon atoms) for the oligomerization of ethylene, whereas the NiMCM-22 catalyst with a microporous structure and a high concentration of acid sites showed lower catalytic activity and selectivity. The balance between acid and nickel ion sites, as well as the textural properties of catalysts, played a significant role in determining their activity and selectivity. In 2014 [62], Ni-*Al*SBA-15 was prepared by the post-synthesis alumination reaction of SBA-15 by sodium aluminate followed by exchanging with nickel ions. The catalyst activity of 175 g/(g<sub>cat</sub>·h) and dimerization selectivity of 77% can be achieved at 150 °C and 35 bar. This catalyst maintains a high and stable conversion rate over eighty hours in a fixed bed reactor at 150 °C, pressure 3.0 MPa, and WHSV 10 h<sup>-1</sup>. This is attributed to the interlinked mesoporous network, which is large enough to allow free diffusion of the product. Shin et al. [63] reported a series of bpy-SBA-15, with different molar amounts of bipyridyl (bpy) sites metalated with NiCl<sub>2</sub>·H<sub>2</sub>O. Bpy-SBA-15 with 0.21 wt% of Ni achieved 4422 mol<sub>oligomers</sub>·mol<sup>-1</sup><sub>Ni</sub>·h<sup>-1</sup> and a selectivity in butene of 77%, with 700 equivalents of Et<sub>2</sub>AlCl. The heterogeneous catalyst can be recycled many times without a significant reduction in catalytic activity due to the stability of the SBA-15 support and the appropriate Ni loading density that reduces the possibility of further reaction of the dimer into polymeric oligomers and polymers. Lacarriere et al. [64] prepared Ni-MCM-41 (Si/Al = 9) by the ion exchange of AlMCM-41 precursors. The catalytic activity of Ni-AlMCM-41 reached 180 g/(g<sub>cat</sub>·h) with a TOF of 16,920 h<sup>-1</sup>, which was far superior to similar Ni-loaded catalysts and comparable to

homogeneous Ni coordination catalysts. Moreover, other molecular sieve catalysts have been used in ethylene oligomerization reactions, like ZSM-5 [65,66], Ni-H-Beta [67,68], and Ni/SIRAL-30 [69], but they did not show desirable linear  $\alpha$ -olefins selectivity.

**Table 1.** A comprehensive contrast of MOFs for olefin oligomerization.

Catalyst	Temperature (°C)	Pressure (bar)	Reaction Time (h)	Co-Catalyst (Al:Ni)	Solvent	Activity or TOF	C <sub>4</sub> (1-C <sub>4</sub> )	C <sub>6</sub>	C <sub>8</sub>	C <sub>8+</sub>	Ref.
Ni-UMOFNS-190 <sup>1</sup>	25	10	1	Et <sub>2</sub> AlCl (500)	toluene	5536 h <sup>-1</sup>	75.6	0.4	22	2	[70]
CPO-27(Ni) <sup>1</sup>	21	10	1	Et <sub>2</sub> AlCl (17)	toluene	1 g/(mol·h)	100				
DUT-8(Ni)-rigid <sup>1</sup>	21	20	1	Et <sub>2</sub> AlCl (17)	toluene	182 g/(mol·h)	76	24			[71]
[Ni(bdc)(dabaco) <sub>0.5</sub> ] <sub>n</sub> <sup>1</sup>	21	10	1	Et <sub>2</sub> AlCl (17)	toluene	41 g/(mol·h)	56	44			
[Ni(bdc)(dabaco) <sub>n</sub> ] <sub>n</sub> <sup>1</sup>	21	10	1	Et <sub>2</sub> AlCl (17)	toluene	41 g/(mol·h)	49	51			
1D-Ni-MIL-77 <sup>1</sup>	30	10	0.5	Et <sub>2</sub> AlCl (100)	toluene	5544 h <sup>-1</sup>	98 (93.3)	0.14		1.84	[72]
3D-Ni-MIL-77 <sup>1</sup>	30	15	0.5	Et <sub>2</sub> AlCl (180)	toluene	2226 h <sup>-1</sup>	99.6 (90)	0.22		0.17	
Ni-ZIF-8 (0.4 wt%) <sup>1</sup>	35	30	0.17	MAO (4640)	toluene	1,116,000 h <sup>-1</sup>	97 (87.7)				[53]
15Ni-ZIF-L <sup>1</sup>	40	30	0.17	MAO	toluene	342,030 h <sup>-1</sup>	96.9 (94.7)				[73]
Ni(1%)-MFU-4l <sup>2</sup>	25	50	1	MAO (500)	toluene	41,500 h <sup>-1</sup>	97.4 (94.5)	2.6			[74]
Ni(7.5%)-CFA-1 <sup>2</sup>	22	50	1	MMAO-12 (2000)	toluene	37,100 h <sup>-1</sup>	95.5 (91.2)				[75]
20Ni-MOF5 (5.32 wt%) <sup>2</sup>	35	50	0.17	MAO	toluene	352,000 h <sup>-1</sup>	96.3 (84.2)				[76]
Ni-AIM-NU-1000 <sup>3</sup>	45	2	10	Et <sub>2</sub> AlCl		1080 h <sup>-1</sup>	42	8	46		[77]
Ni-Facac-AIM-NU-1000	45	2	10	Et <sub>2</sub> AlCl		12.6 h <sup>-1</sup>	100 (78)				[49]
Ni-acac-AIM-NU-1000 <sup>3</sup>	45	2	10	Et <sub>2</sub> AlCl		15.84 h <sup>-1</sup>	100 (82)				
(30)Ni@(Fe)MIL-101 <sup>4</sup>	10	15	1	Et <sub>2</sub> AlCl (70)	heptane	3215 h <sup>-1</sup>	94	5.5	0.5		[78]
MixMOFs-Ni-a <sup>4</sup>	20	20	0.5	Et <sub>2</sub> AlCl (100)	toluene	2071 h <sup>-1</sup>	71.3	6.9	0	21.8	
MixMOFs-Ni-b <sup>4</sup>	40	20	0.5	Et <sub>2</sub> AlCl (100)	toluene	16,428 h <sup>-1</sup>	92.7	6.1	0	1.2	[79]
MixMOFs-Ni-c <sup>4</sup>	20	20	0.5	Et <sub>2</sub> AlCl (100)	toluene	2000 h <sup>-1</sup>	79.5	7.2	0	14.3	
IRMOF-3-Ni-a <sup>4</sup>	20	20	0.5	Et <sub>2</sub> AlCl (100)	toluene	2246 h <sup>-1</sup>	35	9.3	0	55.7	
MIL-125(Ti)-NH <sub>2</sub> (Ni) <sup>4</sup>	50	10	0.5	MAO (800)	cyclohexane	6464 h <sup>-1</sup>	19.6 (87.2)	76.7 (92.5)	1.5	2.2	[54]
NU-1000-bpy-NiCl <sub>2</sub> <sup>4</sup>	21	15	1	Et <sub>2</sub> AlCl (70)	heptane	1560 h <sup>-1</sup>	82	18			[80]
[Al]-Ni-bpydc(MOF) <sup>4</sup>	5	15	1	Et <sub>2</sub> AlCl (70)	heptane	20 g/(g·h)	89.1 (26.3)	8.9	2.1		[81]
[Ni]-Ni-bpydc(MOF) <sup>4</sup>	5	15	1	Et <sub>2</sub> AlCl (70)	heptane	20 g/(g·h)	92.7 (71.3)	7.3			
Zr <sub>6</sub> O <sub>4</sub> (OH) <sub>4</sub> (bpydc) <sub>0.84</sub> (bpdcc) <sub>5.16</sub> (NiBr <sub>2</sub> ) <sub>0.84</sub> <sup>4</sup>	55	59	1	Et <sub>2</sub> AlCl (70)	cyclohexane	370 g/(g/h)					[82]
NiCl@DUT-133 <sup>4</sup>	40	35	1	Et <sub>2</sub> AlCl (51)	1,2-dichlorobenzene	42 mol/(mol·h)	81	19			[83]

<sup>1</sup> Self-assembly. <sup>2</sup> Cation Exchange. <sup>3</sup> Atomic Deposition. <sup>4</sup> Ligand Metalation. 1-olefin is relative to the total amount of oligomer products of that carbon number.

## 2.2.4. Other Materials

Additionally, multiwalled carbon nanotubes (MWCNTs) [84], Ionic Liquid Phase (SILP) [85], clays [86], bispyridine-based porous organic polymers [87], and metal oxides [88,89] have all been studied as carriers of ethylene oligomerization catalysts. These provide new perspectives for the development of new heterogeneous catalysts for ethylene oligomerization.

## 3. Iron-Based Catalysts

### 3.1. Iron-Based Homogeneous Catalysts

Since M. Brookhart [51,90] and V. C. Gibson [91] discovered that iron- and cobalt-based catalysts with bis(imino)pyridine as the ligand have high activity in ethylene oligomerization reaction in 1998, more and more researchers have been attracted to iron-based catalysts. Usually, the activity of iron catalysts is about one order of magnitude higher than that of cobalt catalysts [92]. At the same time, iron has the advantages of large reserves, cheapness, and environmental friendliness, which makes iron catalysts have broad application prospects [93]. In recent years, research on iron-based catalysts for ethylene

oligomerization has mainly focused on ligands [94–96], which could be classified into NNN, NN, NNOO, NNO, and NNNNOO by the element attached to Fe in the ligand. The ligands of iron catalysts are highly modifiable [97–99], and some researchers are devoted to obtaining better catalytic effects by changing the spatial resistances [97,100], substituent groups [101–103], and functional groups [104,105] of the ligands.

### 3.1.1. NNN Ligand

Newly developed ligands and their complexes with iron are not yet comparable to the bis(imino)pyridine system. The latter is still the most promising iron catalyst for industrialization due to its high catalytic activity, high linear selectivity of products, and mild reaction conditions [106,107]. The catalytic activity of the bis(imino)pyridine iron catalyst is even higher than metallocene catalysts, reaching up to  $10^8 \text{ g}\cdot\text{mol}^{-1}\cdot\text{h}^{-1}$ . As shown in Figure 6, the catalyst ligand exhibits a pseudo-tetragonal planar conical geometric configuration, where  $R_1$ – $R_4$  are substituent groups. The two adjacent groups of the benzene ring perpendicular to the metal plane are located, respectively, above and below the plane [108]. The molecular weight of the product can be regulated by modifying the ligand skeleton [109,110] or changing the structure of the benzene ring substituent groups [111].

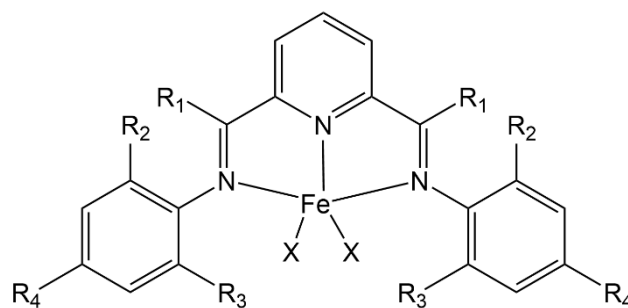


**Figure 6.** Typical structure of bis(imino)pyridine iron catalysts (complex 1). Reproduced with permission from Ref. [108]. Copyright 1999, American Chemical Society.

In addition to the symmetric complexes mentioned above, Xie et al. [112] synthesized a series of 2,6-bis(imino)pyridine Fe(II) asymmetric complexes with alkyl and halogen substituents on different aromatic rings. Compared with symmetric alkyl or halogen substituted complexes, due to their spatial and electronic effects, the proportion of  $C_6$ – $C_{16}$  in oligomers can significantly increase. Claudio Bianchini et al. [113] changed one of the aryliminos in the main chain of bis(imino)pyridine to alkylimino, demonstrating that the presence of two aryl imines in the complex is not a necessary condition for catalytic reactions. The new complexes are effective and selective for the ethylene oligomerization reaction, and the spatial size of alkyl groups can control the catalyst productivity and Schulz–Flory parameters.

Most NNN ligands have good catalytic activity as well as product selectivity. The spatial site resistance of the benzene ring neighboring substituent groups has an effect on the  $\beta$ -H elimination reaction at the catalyst active center. As the steric hindrance decreases, the  $\beta$ -H elimination reaction intensifies, and the molecular weight of the product will significantly decrease. The product is a series of linear  $\alpha$ -olefins when the ortho position of the ligand's aniline group is substituted with a single alkyl group, such as methyl [114].

### 3.1.2. NN Ligand

For NN ligands, Zhang et al. [115] synthesized a novel star iminopyridyl iron complex using 1.0 G star macromolecule, pyridine-2-carboxaldehyde, and  $\text{FeCl}_2\cdot 4\text{H}_2\text{O}$  as raw materials. After activation by MAO, this complex exhibits high ethylene oligomerization activity ( $7.5 \times 10^4 \text{ g}\cdot\text{mol}^{-1}\cdot\text{Fe}\cdot\text{h}^{-1}$ ) while achieving a selectivity of 70.69% for butene. Higher catalytic activity can be obtained by increasing the ethylene pressure and Al/Fe molar ratio.

### 3.1.3. NNOO Ligand

Zhang et al. [116] synthesized a series of novel hyperbranched salicylaldimine Fe(II) complexes. The catalytic activity and product selectivity of ethylene oligomerization, which uses MAO as co-catalyst and toluene as solvent, can be modified by changing reaction temperature, ethylene pressure, and Al/Fe molar ratio. Under optimal conditions ( $[Fe] = 7 \text{ mmol}$ ,  $298 \text{ K}$ ,  $Al/Fe = 500$ ,  $0.5 \text{ MPa}$  ethylene), the catalytic activity can reach  $6.91 \times 10^4 \text{ g}\cdot\text{mol}^{-1}_{Fe}\cdot\text{h}^{-1}$ , and the selectivity for higher-carbon-number olefins ( $C_{10+}$ ) is 20.48%. Li et al. [117] synthesized iron complexes based on hyperbranched salicylaldimine ligands for ethylene oligomerization reaction. After activation with MAO, the activity of the catalyst reached  $13.5 \times 10^4 \text{ g}\cdot\text{mol}^{-1}_{Fe}\cdot\text{h}^{-1}$ , and the proportion of  $C_4$  in the product reached 52.1%, while the proportion of  $C_8$  reached 32.63%.

### 3.1.4. NNO Ligand

George S. Nyamato et al. [118] synthesized (Pyrazolyl)-(phosphinoyl)pyridine iron(II) complex for ethylene oligomerization. Figure 7 shows the molecular structures and synthesis of (pyrazolyl)-(phosphinoyl)pyridine Fe(II), Co(II), and Ni(II) complexes. Compounds 2–7 in Figure 7 were activated with  $\text{EtAlCl}_2$ , MAO, or  $\text{AlMe}_3$  as co-catalysts, and  $\alpha\text{-C}_4$  was obtained as the main product in the ethylene oligomerization reaction using hexane, chlorobenzene, or toluene as solvents. The catalytic activity and product selectivity depend largely on the nature of the alkylaluminium co-catalyst, the nature of the solvent, and the complex structure. Despite the low activity of this catalyst, it has the advantage of high selectivity for  $\alpha$ -linear olefins.

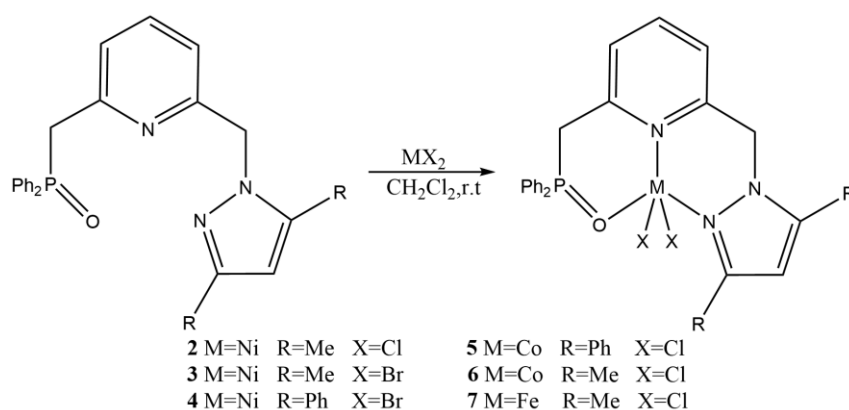


**Figure 7.** Molecular structures and synthesis of (pyrazolyl)-(phosphinoyl)pyridine Fe(II), Co(II), and Ni(II) complexes. Reprinted from Journal of Organometallic Chemistry, 783, Nyamato et al., (Pyrazolyl)-(phosphinoyl)pyridine iron(II), cobalt(II) and nickel(II) complexes: Synthesis, characterization and ethylene oligomerization studies, pp. 64–72. Copyright (2015), with permission from Elsevier [118].

### 3.1.5. NNNNOO Ligand

Makhosonke Ngcobo et al. [93] synthesized Fe(II) complex of bidentate and tridentate (imino)phenol ligands bearing quinoline motifs (Figure 8). Using chlorobenzene as solvent, complex 8 undergoes ethylene oligomerization reaction under the activation of  $\text{EtAlCl}_2$ . Under the optimal reaction conditions, the catalytic activity reached  $6.84 \times 10^5 \text{ g}\cdot\text{mol}^{-1}_{cat}\cdot\text{h}^{-1}$ . The selectivity of  $C_4$  ( $\alpha\text{-C}_4$ ) and  $C_6$  ( $\alpha\text{-C}_6$ ) in the oligomers is 65% (93%) and 35% (19%), respectively.

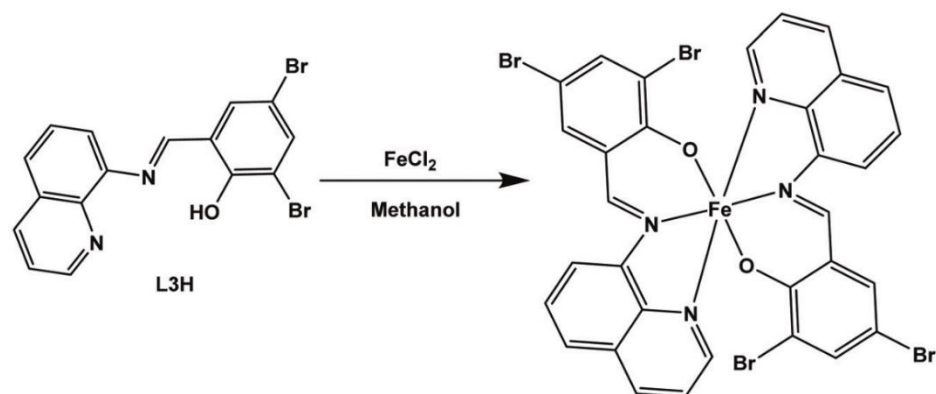


**Figure 8.** Molecular structures and the synthesis route of Fe(II) complexes of bidentate and tridentate (imino)phenol ligands bearing quinoline motifs (complex **8**).

### 3.2. Iron-Based Heterogeneous Catalyst

Fe-based homogeneous catalysts exhibit high activity and good selectivity in ethylene oligomerization. Although a better catalytic effect can be achieved by changing the spatial site resistance, substituent group, and functional group of the ligand for the complexes, their industrial application is limited owing to the difficulty of separating the catalyst from the products [119,120] and the large amount of heat released during the reaction process [121,122]. Moreover, the products of most catalytic systems are  $C_4$  or  $C_6$ . In recent years, there has been an increasing number of studies on the immobilization of homogeneous catalysts on inorganic supports, such as zeolites [120], silica [123–125], and organic polymers [126,127].

In the study of heterogeneous ethylene oligomerization, the key aspect of effective catalyst design involves the isolated active metal sites within mesoporous support materials. Metal–organic frameworks (MOFs) are materials possessing a large surface area and a highly ordered porous structure, which can be used as effective catalysts for ethylene oligomerization reaction. The products of ethylene oligomerization catalyzed by iron catalysts generally have low carbon numbers. However, Yang Han et al. [128] synthesized MIL-100(Fe) via a hydrothermal method, which can catalyze ethylene tetramerization to produce  $C_8$  liquid products under mild reaction conditions. The proportion of  $C_8$  liquid products is over 70%, but the proportion of  $\alpha$ -olefins is very low, only at 3%. Three conditions affect the catalytic activity of MIL-100(Fe): the surface area, the  $Fe^{2+}/Fe^{3+}$  ratio, and the vacuum activation temperature. Temperature changes the  $Fe^{2+}/Fe^{3+}$  ratio in the catalyst, and the relationship between temperature and catalytic activity is volcanic. Meanwhile, different co-catalysts affect the product distribution. The  $C_8$  product selectivity was 75% when  $Et_2AlCl$  or MAO were used as co-catalysts. However, when  $Et_3Al$  was used as a co-catalyst, the  $C_8$  product selectivity in the product was only 43.73%.

One way to synthesize loaded catalysts is to immobilize homogeneous catalysts directly onto the support. In 2002, Franz A. R. Kaul et al. [129] immobilized bis(imino)pyridyliron(II) complexes on silica. In recent years, Arumugam Jayamani et al. [125] immobilized Fe(II) catalysts chelated by (phenoxy)imine ligand on MCM-41. The series of catalysts demonstrated high ethylene oligomerization activity with  $EtAlCl_2$  as a co-catalyst and toluene as a solvent. The catalytic activity of the homogeneous catalyst was  $1.84 \times 10^5 \text{ g}\cdot\text{mol}^{-1}_{\text{cat}}\cdot\text{h}^{-1}$ . Meanwhile, the heterogeneous catalyst using MCM-41 to immobilize the complex presented catalytic activity of  $0.97 \times 10^5 \text{ g}\cdot\text{mol}^{-1}_{\text{cat}}\cdot\text{h}^{-1}$  under the same reaction conditions. The catalytic activity of the catalyst is relatively low after immobilization due to the large spatial site resistance, which limits the binding between ethylene and the metal active centers. In the two cycling experiments, there was almost no decrease in catalytic activity, and the product distribution remained unchanged, so the nature of the active species in the catalyst did not change during the cycling experiments.

Makhosonke Ngcobo et al. [130] synthesized loaded catalysts after the phenol ((tri-ethoxysilyl)propylimino) ligand was immobilized onto SBA-15 or MCM-41 and reacted with  $\text{FeCl}_2$ . The ethylene oligomerization reaction catalyzed by the materials with  $\text{EtAlCl}_2$  as a co-catalyst provided mainly  $\text{C}_6$  oligomers (92% selectivity using Fe-SBA-15 catalyst). Because the ethylene oligomerization reaction occurs in the pores of the support and the pore size of SBA-15 is larger than that of MCM-41, and large pore size reduces the mass transfer resistance, Fe-SBA-15 was more active than Fe-MCM-41 in the reaction. The catalytic activity of Fe-SBA-15 decreased by 30% after two cycling experiments, and the selectivity for the product  $\text{C}_6$  was maintained at 92%. The authors attribute the decrease in activity to the loss of active metal atoms and structural changes in the support. It is interesting that this research group previously immobilized homogeneous catalysts onto  $\text{Fe}_3\text{O}_4$  magnetic nanoparticles to obtain recyclable catalysts [131]. Utilizing the ferromagnetism of the support, the catalyst can be easily separated from the reaction mixture via an external magnet and reused.

Another way to prepare loaded catalysts is to immobilize homogeneous catalysts onto a support that was pretreated by MAO or aluminum alkyls. Guo et al. [107] immobilized bis(imino)pyridine iron complexes on mesoporous molecular sieves (MCM-41 and SBA-15). Prior to this, the mesoporous molecular sieves need to be dried under vacuum at 393 K to constant weight and then refluxed with MAO overnight. During pretreatment, MAO chemically binds to the silanol groups on the inner walls of MCM-41 or SBA-15, so there is no need to add MAO as a co-catalyst during the ethylene oligomerization. The activators and monomer molecules are required to approach metal active sites in the reaction, and pores limit the process. After immobilization, the incidences of chain termination and transfer also increase. So, the loaded catalysts can lead to lower activity and lower carbon number products. Due to the smaller pore size of MCM-41 compared to SBA-15, this phenomenon is more pronounced in the former. Temperature also affects the product distribution of the reaction, and the increase in temperature accelerates the  $\beta$ -H elimination reaction, resulting in a higher proportion of products with low molecular weight. The group also used mesoporous molecular sieves modified with MAO as a support, loaded with iron-based diimine complexes, to catalyze the ethylene oligomerization to produce low-carbon-number  $\alpha$ -olefins [124]. Under the same conditions, the catalytic activity of the complex reached  $6.06 \times 10^6 \text{ g}\cdot\text{mol}^{-1}_{\text{Fe}}\cdot\text{h}^{-1}$ , while that of the loaded type was only  $4.35 \times 10^6 \text{ g}\cdot\text{mol}^{-1}_{\text{Fe}}\cdot\text{h}^{-1}$ .

## 4. Cobalt-Based Catalysts

### 4.1. Cobalt-Based Homogeneous Catalysts

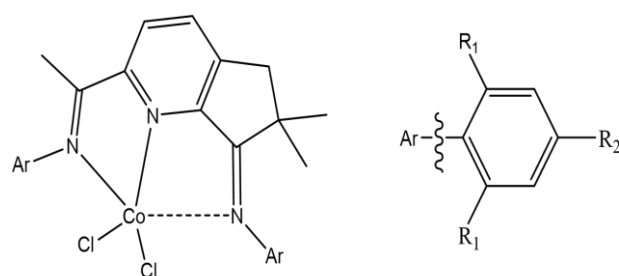
Late transition metal cobalt, nickel, and iron are generally used in the oligomerization or dimerization of ethylene. These metals have more d electrons, larger ionic radii, and easier access to ligands, resulting in the formation of catalysts with a strong tendency for  $\beta$ -H elimination. Nickel- and iron-based catalysts are discussed, and then this section will introduce the cobalt-based catalysts employed for ethylene oligomerization over the past decade, which are summarized in terms of the denticity (tri-dentate, bi-dentate, and other types) of the ligands.

#### 4.1.1. Tri-Dentate Cobalt Complex

The tri-dentate-coordinated cobalt catalysts showed good catalytic activity in this reaction, and there has been much progress in this area in recent years.

Sun et al. [132] investigated cobalt complexes 9–12 (Figure 9) bearing 2-(1-(arylimino)ethyl)-7-arylimino-6,6-dimethylcyclopentapyridine for ethylene oligomerization. The molecular structures indicate that 2,7-bis(aryl)cyclopentapyridines is a tridentate ligand; however, one of the Co-N coordination bonds is weak due to the spatial separation of the nitrogen atom. Upon activation by MAO or MMAO, all the cobalt complexes exhibited catalytic activity toward ethylene oligomerization. Under the activation of MMAO, the oligomerization process was highly selective for  $\alpha$ -olefins, and the result-

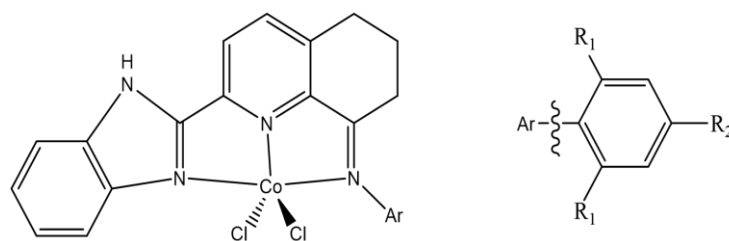
ing oligomers fully complied with the Schulz–Flory rule. Later, this group successfully synthesized cobalt(II) chloride complexes **13–18** (Figure 10) by a one-pot reaction of 2-benzoimidazolyl-5,6,7-trihydroquinolin-8-one with the corresponding aniline in the presence of cobalt dichloride [133]. Upon activation by MAO, all the complexes were effective in catalyzing the dimerization of ethylene, and especially the activity of compound **16** reached  $1.23 \times 10^5 \text{ g} \cdot \text{mol}^{-1} \cdot \text{Co} \cdot \text{h}^{-1}$ , producing products dominated by 1-butene. In contrast, with MMAO as the co-catalyst, the trimerization process of this system was superior, with selectivity for 1-hexene up to 49% (with complexes **15** and **17**). Ortho-benzhydryl-substituted 2-imino-1,10-phenanthroline cobalt complexes **19–26** were also synthesized and characterized by this group (Figure 11) [134]. In the presence of methylaluminoxane (MMAO), all the cobalt complexes showed good ethylene dimerization activity (up to  $3.25 \times 10^5 \text{ g} \cdot \text{mol}^{-1} \cdot \text{Co} \cdot \text{h}^{-1}$  at 50 °C), and the selectivity of C<sub>4</sub> was distributed from 92% to 100%, in which the selectivity of 2-butene ranged from 55 to 84.4%. The reason may be that the steric hindrance environment around the cobalt atom is less, which is favorable for the cis–trans conformational rearrangement of C–H.



**9** R<sub>1</sub> = Me R<sub>2</sub> = H **11** R<sub>1</sub> = Me R<sub>2</sub> = Me

**10** R<sub>1</sub> = Et R<sub>2</sub> = H **12** R<sub>1</sub> = Et R<sub>2</sub> = Me

**Figure 9.** Structure of cobalt complexes **9–12**.



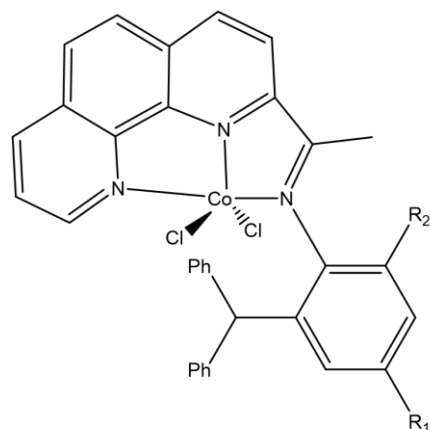
**13** R<sub>1</sub> = Me R<sub>2</sub> = H **16** R<sub>1</sub> = Me R<sub>2</sub> = Me

**14** R<sub>1</sub> = Et R<sub>2</sub> = H **17** R<sub>1</sub> = Et R<sub>2</sub> = Me

**15** R<sub>1</sub> = iPr R<sub>2</sub> = H **18** R<sub>1</sub> = t-Bu R<sub>2</sub> = t-Bu

**Figure 10.** Structure of cobalt complexes **13–18**.

Konstantin P. Bryliakov and co-workers [135] prepared a series of novel cobalt(II) bis(imino) pyridine complexes bearing one or several electron-withdrawing substituents at the aniline moieties (Figure 12). Activated by MAO, the ethylene oligomerization activity of these complexes reached  $1.8 \times 10^7 \text{ g}_{\text{products}} \cdot \text{mol}^{-1} \cdot \text{Co} \cdot \text{h}^{-1} \cdot \text{bar}^{-1}$ . Cobalt complexes **29**, **31**, **32**, and **34** with electron-withdrawing substituents (Cl or CF<sub>3</sub>) showed higher catalytic activity (Table 2). Depending on the nature and number of electron-withdrawing groups, the process presents the selectivity ranges from dimerization (up to 98% for 1-butene) to oligomerization (C<sub>4</sub>–C<sub>12+</sub>) and is accompanied by the formation of strictly linear low-molecular-weight polyethylene.



- 19**  $R_1 = \text{Me}$   $R_2 = \text{CH}(\text{Ph})_2$  **23**  $R_1 = \text{CH}(\text{Ph})_2$   $R_2 = \text{Me}$   
**20**  $R_1 = \text{Et}$   $R_2 = \text{CH}(\text{Ph})_2$  **24**  $R_1 = \text{CH}(\text{Ph})_2$   $R_2 = \text{Et}$   
**21**  $R_1 = \text{iPr}$   $R_2 = \text{CH}(\text{Ph})_2$  **25**  $R_1 = \text{CH}(\text{Ph})_2$   $R_2 = \text{iPr}$   
**22**  $R_1 = \text{Cl}$   $R_2 = \text{CH}(\text{Ph})_2$  **26**  $R_1 = \text{CH}(\text{Ph})_2$   $R_2 = \text{CH}(\text{Ph})_2$

**Figure 11.** Ortho-benzhydryl-substituted 2-imino-1,10-phenanthroline cobalt complexes **19–26**.

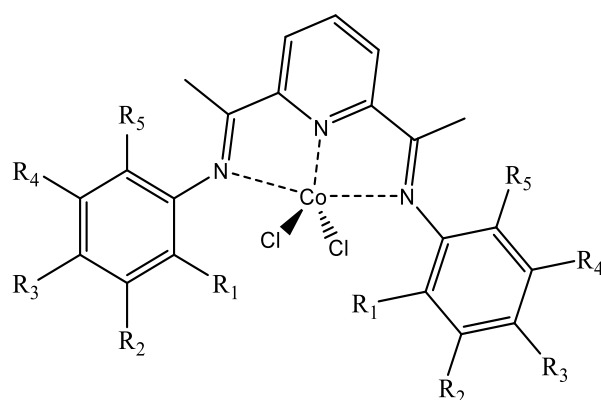


**Figure 12.** Cobalt(II) bis(imino) pyridine complexes bearing one or several electron-withdrawing substituents at the aniline moieties. Reprinted from Journal of Organometallic Chemistry, 884, Antonov et al., Catalytic ethylene oligomerization on cobalt(II) bis(imino)pyridine complexes bearing electron-withdrawing groups, pp. 55–58. Copyright (2019), with permission from Elsevier [135].

**Table 2.** The types of  $R_1$ – $R_5$  substituents of Cobalt(II) bis(imino) pyridine complexes in Figure 12.

Complex	$R_1$	$R_2$	$R_3$	$R_4$	$R_5$
<b>27</b>	H	H	F	H	H
<b>28</b>	H	H	Br	H	H
<b>29</b>	Cl	H	F	H	H
<b>30</b>	F	H	H	H	H
<b>31</b>	H	Cl	H	Cl	H
<b>32</b>	$\text{CF}_3$	H	H	H	H
<b>33</b>	H	F	H	F	H
<b>34</b>	$\text{CF}_3$	H	F	H	H
<b>35</b>	H	$\text{CF}_3$	F	H	H
<b>36</b>	F	H	F	H	F
<b>37</b>	Cl	H	H	H	Cl
<b>38</b>	H	Cl	H	H	H
<b>39</b>	Br	H	H	H	H
<b>40</b>	Me	H	H	H	Me

#### 4.1.2. Bi-Dentate Cobalt Complex

Bi-dentate ligand cobalt catalysts tend to exhibit relatively low ethylene reactivity compared to tri-dentate ligand cobalt catalysts. Such low activity is probably due to the formation of unstable active species. The metal sites possess greater open spaces and tend to be more prone to coordinate with other species present in the system (leading to deactivation).

N<sup>^</sup>N bi-dentate ligand cobalt complexes were found to exhibit high activity and selectivity for dimerization. Katia et al. [136] investigated three cobalt-β-diimine complexes **41–43** (Figure 13) for ethylene oligomerization. At 10 bar, 30 °C, using EASC as a co-catalyst and toluene as a solvent, complex **42** exhibited the highest activity (TOF = 34 s<sup>-1</sup>), while the TOF of complex **43** was only 0.8 s<sup>-1</sup>. More charge on the center metal leads to higher catalytic activity, so complex **42** with two electron-donating methoxy groups possesses the highest activity. The selectivity of complexes **42** and **43** remained the same, with about 70% selectivity for C<sub>4</sub>. Wang et al. [137] synthesized N,N-bidentate iron, nickel, and cobalt complexes bearing (6E,7E)-N<sup>1</sup>,N<sup>4</sup>-bis((pyridin-2-yl)methylene)benzene-1,4-diamine ligands and investigated their ethylene oligomerization potential. The selectivity toward 1-hexene for cobalt complex **44** was usually higher than that of the iron or nickel complexes at 40 bar pressure. The authors inferred that the N–M–N bite angle had an effect on the catalytic selectivity, and the small N–M–N bite angle produced high-carbon olefins. Another group [115], in 2022, synthesized a novel star iminopyridyl cobalt with 1.0 generation (1.0 G) star macromolecule and pyridine-2-carboxaldehyde as the raw materials. In the presence of methylalumoxane (MAO), cobalt complex **45** demonstrated higher ethylene oligomerization activity (up to 4.28 × 10<sup>5</sup> g·mol<sup>-1</sup>Co·h<sup>-1</sup>), affording C<sub>4</sub> as the major product as well as C<sub>6</sub>, C<sub>8</sub>, and C<sub>10–18</sub> oligomers. Sun et al. [138] reported dinuclear pyridyl-imine Co-based complexes **46** and **47** prepared through the one-pot synthesis method. Complexes **46** and **47**, activated by MMAO, were capable of producing ethylene oligomers with moderate activity (up to 5.1 × 10<sup>5</sup> g·mol<sup>-1</sup>Co·h<sup>-1</sup> for complex **47**) in which α-C<sub>8</sub> was the major product.

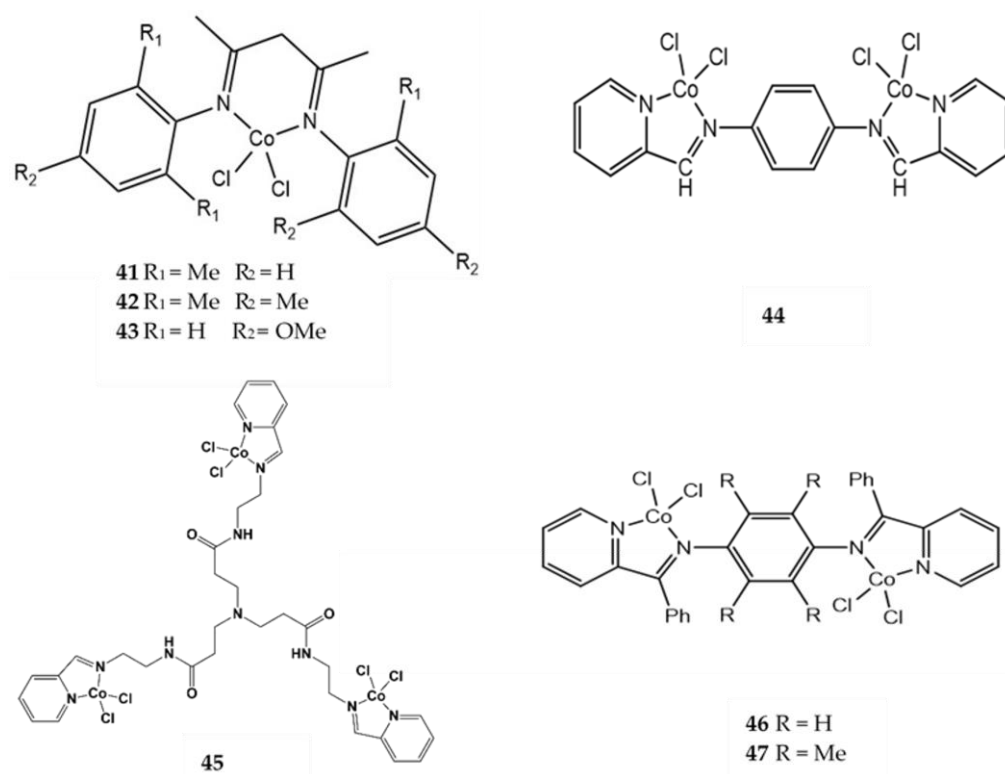


Figure 13. Structure of cobalt complexes 41–47.

Jiang and co-workers [139] reported a series of cobalt complexes featuring a monomeric structure with the silicon-bridged diphosphine ligand to the cobalt center (Figure 14). Transition metals supported with diphosphine ligands can exhibit good catalytic performance due to their singly and weakly coordinating moieties that can readily dissociate to create a vacant site for coordination, thereby enhancing the catalytic activity [140,141]. Changing the N-substituent from the larger 2,6-diisopropylphenyl to the smaller cyclopentyl and isopropyl moieties resulted in a decrease in the selectivity of 1-butene from 79.5% to 32.4 and 27.4%, respectively. Under optimal conditions, complex **48** exhibited the highest ethylene dimerization activity ( $2.3 \times 10^5 \text{ g}\cdot\text{mol}^{-1}\text{Co}\cdot\text{h}^{-1}$ ), providing 100% selectivity toward  $\text{C}_4$  and 78.6% selectivity toward 1-butene.

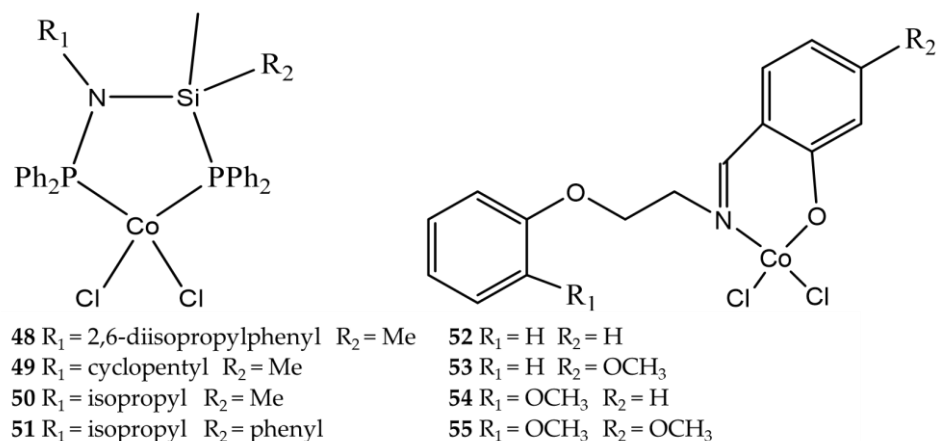
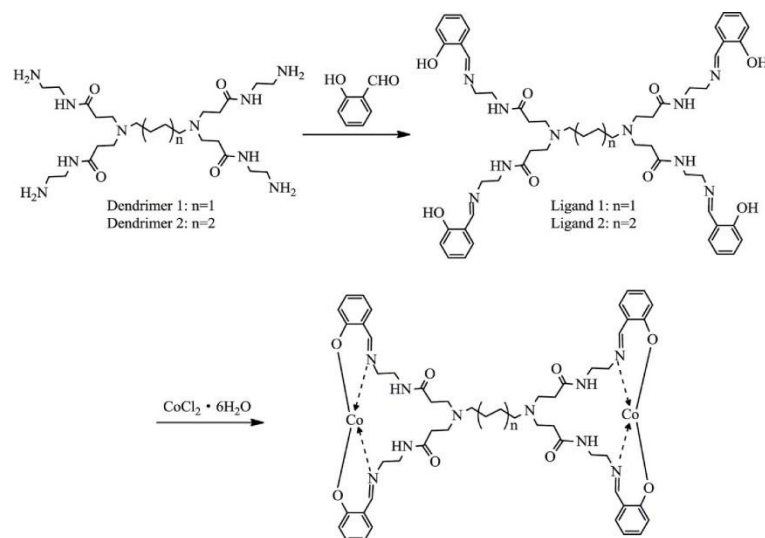


Figure 14. Structure of cobalt complexes 48–55.

Wang and co-workers [25] explored a series of cobalt complexes as catalyst precursors and reported their performance in the ethylene oligomerization with MAO as an activator (Figure 14). Under the optimum conditions ( $n$  (catalyst) =  $7 \mu\text{mol}$ ,  $T = 50 \text{ }^\circ\text{C}$ ,  $P$  (ethylene pressure) =  $2.0 \text{ MPa}$ ,  $n(\text{Al})/n(\text{M}) = 300$ , toluene as solvent), complex **55** produced the selectivity of 34.44% to  $\text{C}_8$  and activity of  $3.38 \times 10^5 \text{ g}\cdot\text{mol}^{-1}\text{Co}\cdot\text{h}$ . In this system, the catalytic performance of the cobalt complex is better than that of the nickel complex.

#### 4.1.3. Other Types of Cobalt Complex

Salicylaldimine ligands, a kind of Schiff base, have the ability to coordinate to metals via hard nitrogen and oxygen donor atoms, which results in metal complexes with better anti-reductive stability and unusual thermal stability. Wang et al. [142] synthesized two cobalt complexes based on dendritic PAMAM-bridged salicylaldimine ligands (Figure 15). After EASC activation at  $1.0 \text{ MPa}$ ,  $25 \text{ }^\circ\text{C}$ , and an Al/Co molar ratio of 1500, the highest catalytic activity and selectivity of complex **50** for  $\text{C}_{10}\text{--C}_{20}$  were  $3.44 \times 10^6 \text{ g}\cdot\text{mol}^{-1}\text{Co}\cdot\text{h}^{-1}$  and 76.53%, respectively; and the highest catalytic activity and selectivity of complex **57** for  $\text{C}_{10}\text{--C}_{20}$  were  $3.42 \times 10^6 \text{ g}\cdot\text{mol}^{-1}\text{Co}\cdot\text{h}^{-1}$  and 84.50%. Another group [143], in 2016, explored three cobalt complexes (**58–60**) bearing hyperbranched salicylaldimine ligands with tetradecyl, hexadecyl, or octadecyl as cores (Figure 16). Under the same reaction conditions, it is obvious that the catalytic activity decreases ( $58 > 59 > 60$ ) with the increase in the length of the alkyl chain in the skeleton, but it has little effect on the selectivity of the products. The main reason for the decrease in activity is that the bulkier ligand hinders the coordination of ethylene to the active metal center, resulting in a lower insertion rate of ethylene. Later, the group synthesized a series of 1.0 G hyperbranched macromolecules bridged salicylaldimine cobalt complexes using 1.0 G hyperbranched macromolecules, salicylaldehyde, and cobalt chloride hexahydrate as raw materials (Figure 17) [144]. To summarize the three types of cobalt complexes of salicylaldimine ligands mentioned above, the backbone structure affects the activity and product selectivity of ethylene oligomerization.



**Figure 15.** Structure of cobalt complexes **56** ( $n = 1$ ) and **57** ( $n = 2$ ). Cobalt complexes based on dendritic PAMAM bridged salicylaldimine ligands: Synthesis, characterization and performance in ethylene oligomerization, [142] *Journal of Macromolecular Science, Part A: Pure and Applied Chemistry*, 29 September 2016, reprinted by permission of the publisher (Taylor & Francis Ltd., accessed on 12 March 2024, <http://www.tandfonline.com>).

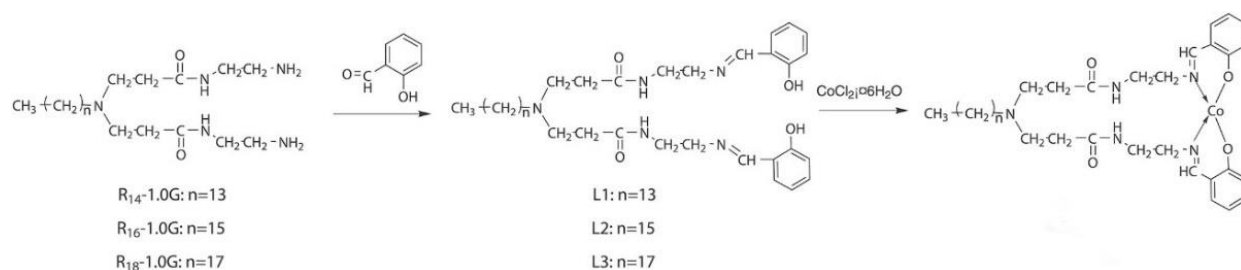


**Figure 16.** Structure of cobalt complexes **58** ( $n = 13$ ), **59** ( $n = 15$ ), and **60** ( $n = 17$ ) bearing hyperbranched salicylaldimine ligands. Reproduced from Ref. [143] with permission from WILEY.

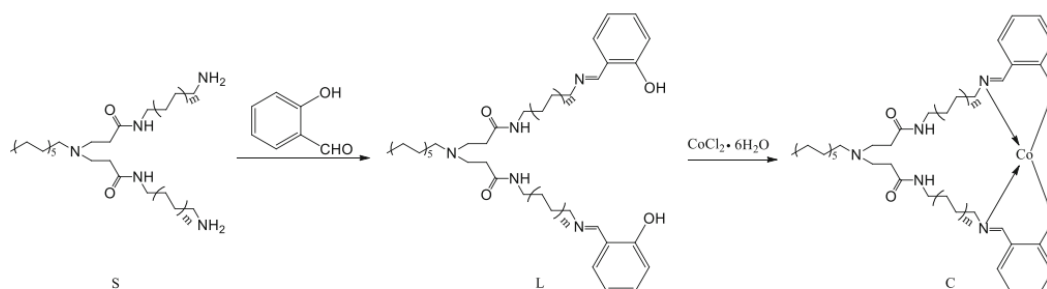


**Figure 17.** Structure of cobalt complexes **61** ( $m = 0$ ), **62** ( $m = 1$ ), **63** ( $m = 2$ ), and **64** ( $m = 3$ ). Hyperbranched macromolecules bridged salicylaldimine cobalt complexes: synthesis, characterization and ethylene oligomerization studies, Zhang et al., *Chem. Pap.*, 71:1037–1046, Springer Nature, 2017, reproduced with permission from SNCSC [144].

Stephen O. Ojwach et al. [145] reported Co(II) complexes of 2-[(ethylimino) methyl] phenol ligands as potential catalysts for ethylene oligomerization reactions (Figure 18). The authors established multiple coordination modes of Co(II) complexes that are dependent on the N<sup>∞</sup>O ligand. The ligands of these mono- and dinuclear complexes employ tri/di-dentate coordination. Under MAO activation, these cobalt complexes produce mainly C<sub>4</sub> (up to 96%), while C<sub>6</sub> is the main product under EtAlCl<sub>2</sub> activation. The Co(II) complex of bidentate and tridentate (imino)phenol ligands bearing pyridine and quinoline motifs

was also successfully synthesized by this group [93]. The activation of the Co(II) complex by  $\text{EtAlCl}_2$  co-catalysts makes it active in ethylene oligomerization reactions to produce mainly  $\text{C}_4$  and  $\text{C}_6$  oligomers.

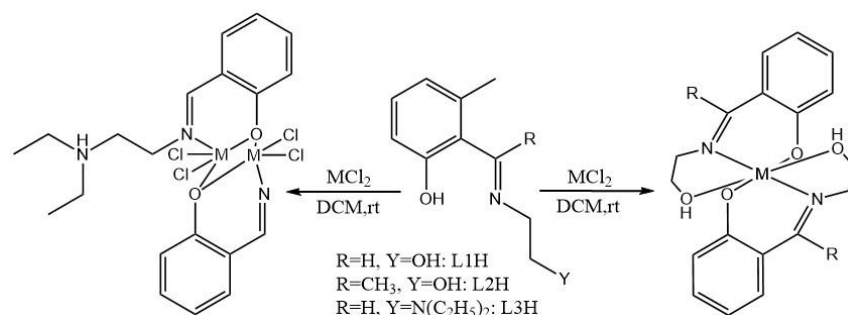


**Figure 18.** Synthetic protocol of  $\text{N}^{\text{O}}$  donor (ethylimino)methylphenol Co(II) complexes (right: complex **65**  $\text{R} = \text{H}$  and complex **66**  $\text{R} = \text{CH}_3$ ; left: complex **67**). Reprinted from Molecular Catalysis, 478, Ngcobo et al., Structural elucidation of  $\text{N}^{\text{O}}$  (ethylimino-methyl)phenol Fe(II) and Co(II) complexes and their applications in ethylene oligomerization catalysis, p. 110590, Copyright (2019), with permission from Elsevier [145].

Sergey V. Zubkevich et al. [146] designed a novel tetradentate NNNO-heteroscorpionate ligand with an 8-methoxyquinoline pendant arm and synthesized monomeric molecular complex Co(II) halides with it. The complex was inactive under organoaluminum compounds (such as MAO,  $\text{EtAl}_3$ , etc.) activation, while, under  $\text{Et}_2\text{AlCl}$  or  $\text{Et}_3\text{Al}_2\text{Cl}_3$  activation, the cobalt complexes have a moderate activity of  $60\sim 130 \text{ kg}_{\text{oligomer}} \cdot \text{mol}^{-1}_{\text{Co}} \cdot \text{h}^{-1} \cdot \text{atm}^{-1}$  in solvent of toluene and form a mixture of butene and hexene with an  $\alpha$ -olefin percentage (1-butene and 1-hexene) of more than 70%. The higher activity ( $140$  to  $200 \text{ kg}_{\text{oligomer}} \cdot \text{mol}^{-1}_{\text{Co}} \cdot \text{h}^{-1} \cdot \text{atm}^{-1}$ ) of the catalyst in chlorobenzene is mainly due to the better solubility of the cobalt complex in polar solvents.

#### 4.2. Cobalt-Based Heterogeneous Catalysts

Compared to homogeneous cobalt catalysts, heterogeneous cobalt catalysts have progressed very slowly regarding the ethylene oligomerization reaction. One important reason is that the catalytic activity of heterogeneous cobalt catalysts is lower than that of heterogeneous nickel catalysts.

In recent years, the chemical functionalization of carbon nanotubes (CNTs) with metal complexes has become one of the promising directions for materials development in various fields. Norah Alhokbany [84] reported the preparation of pyridylimino cobalt complex-functionalized multiwalled carbon nanotubes [Pyr-Co(II) MWCNTs] and their catalytic activity for ethylene oligomerization after activation by methylaluminoxane (MAO). The activity and selectivity of this catalyst was found to be sensitive to pressure and the Al/Co ratio. When the amount of co-catalyst is low, it exhibits moderate catalytic activity as well as a predominant selectivity to  $\text{C}_{10}\text{--}\text{C}_{12}$ .

Heterogeneous carbon-supported cobalt catalysts have become an important branch of the ethylene oligomerization reaction. Xu et al. [147] demonstrated that  $(\text{CoO}_x/\text{N-C})$ , in a continuous-flow reactor at  $80^\circ\text{C}$ , produced octene with linearity of 77.6% in the ethylene oligomerization reaction, but 1-octene was only 5.2% at 20% conversion. Xu et al. [148] further claimed that incorporation of Cr into the cobalt oxide on a carbon catalyst ( $\text{Cr-CoO}_x/\text{N-C}$ ) improved the catalytic activity and stability in the ethylene oligomerization reaction at  $80^\circ\text{C}$ . Alvin Jonathan et al. [149] reported that cobalt oxide on a carbon catalyst is more stable at higher temperatures ( $\sim 200^\circ\text{C}$ ), likely due to the reduction of  $\text{Co}_3\text{O}_4$  to  $\text{CoO}$ , while rapid deactivation is observed at lower temperatures (e.g.,  $80\text{--}140^\circ\text{C}$ ). At a reaction temperature of  $200^\circ\text{C}$ , the catalyst was highly selective for linear olefins, including linear  $\alpha$ -olefins. At 48.3% ethylene conversion, the product linearity can reach more than 90%; at low conversion of 20%, the product linearity can reach 60%. Another group [150] demonstrated that increasing the catalyst pretreatment temperature from

230 °C to 560 °C in an argon atmosphere reduces cobalt oxide to cobalt metal and increases activity. However, the Co metal on the carbon catalyst was deactivated owing to the formation of polyethylene on the catalyst (the spent catalyst contained approximately 50 wt% polyethylene after 24 h of reaction). The catalyst support has an effect on the cobalt catalyst for ethylene oligomerization to generate linear olefins [151]. The high-temperature-treated carbon-supported cobalt oxide catalyst (CoO<sub>x</sub>/MRX-HTTC) was almost twice as active as the acid-washed carbon-supported cobalt oxide catalyst (CoO<sub>x</sub>/MRX-AWC), with more linear alpha olefins. Acid wash treatment oxidizes the surface functional groups and increases the oxygen content of the carbon support, leading to the isomerization of linear  $\alpha$ -olefins into linear internal olefins. Zhong et al. [152] investigated the structure-performance evolution of the Co/NAC catalyst for ethylene oligomerization in detail. The initial ethylene conversion was as high as 64%, but it was quickly deactivated and the conversion dropped to 4% after 30 h of reaction. Butene dominated the product, and its selectivity gradually increased in the first 10 h, and then remained at about 74%.

UiO-66-NH<sub>2</sub>-grafted pyridinimine ligand [153] was prepared by a post-synthetic modification method using metal-organic skeletons (MOFs) UiO-66-NH<sub>2</sub> and pyridine 2-formaldehyde as raw materials, and then it reacted with CoCl<sub>2</sub>·6H<sub>2</sub>O to obtain the UiO-66-NH<sub>2</sub>-grafted pyridinimine cobalt catalyst. When cyclohexane was used as the solvent and methylaluminoxane (MAO) as the co-catalyst, the activity of the catalyst for the oligomerization of ethylene could reach  $1.23 \times 10^5 \text{ g}\cdot\text{mol}^{-1}\text{Co}\cdot\text{h}^{-1}$ , and the selectivity for butylene was 88.96% at a pressure of 10 bar using the molar ratio [Al/Co] of 1000:1 at 25 °C.

Stephen O. Ojwach et al. [125] immobilized 2-phenyl-2-((3(triethoxysilyl)propyl)imino)ethanol(L1) or 4-nitro-2-((3(triethoxysilyl)propyl)imino)methyl)phenol(L2) on an MCM-41 support and then reacted with CoCl<sub>2</sub>. The immobilized catalysts were active regarding the ethylene oligomerization, while their activity was lower than that of the homogeneous compounds. There was no significant loss regarding the catalytic activity or leaching of active substances in three runs.

## 5. Chromium-Based Catalysts

### 5.1. Chromium-Based Homogeneous Catalysts

For the catalytic systems mentioned above, it is generally believed that the ethylene oligomerization processes are in compliance with the ethylene insertion/ $\beta$ -H elimination mechanism (Cossee chain growth mechanism). Thus, the reaction products are all mixtures of a range of olefins, consistent with the Schulz–Flory distribution. However, Cr-based catalysts follow the metallacyclic mechanism and mainly catalyze selective ethylene tri-/tetramerization reactions. In recent years, there have been many reports of Cr-based catalysts in the ethylene oligomerization process owing to their high activity [154–156], high selectivity [157,158], and diversity of ligand structures [159–161].

#### 5.1.1. Ethylene Trimerization

As early as 1967, Manyik [162] found the presence of a small amount of 1-hexene in the product of ethylene polymerization catalyzed by chromium(III) 2-ethylhexanoate and partially hydrolyzed triisobutylaluminum. In 1976, Manyik et al. first proposed the metallacyclic mechanism for the selective ethylene trimerization by Cr-based catalysts. Briggs [1] optimized the chromium(III) 2-ethylhexanoate system using dimethoxyethane in 1989 to promote the trimerization of ethylene to form 1-hexene and verified the metallacyclic mechanism that forms a seven-membered ring intermediate from chromium atoms and three ethylene molecules followed by reductive elimination to produce 1-hexene. Chevron Phillips proposed an efficient catalytic ethylene trimerization using an activator consisting of dichloroethylaluminum or triethylaluminum with chromium(III)2-ethylhexanoate combined in situ with 2,5-dimethylpyrrole as the ligand in 1996. This catalytic system can reach an activity value of  $3.019 \text{ kg}\cdot\text{mol}^{-1}\cdot\text{h}^{-1}$ ) and selectivity of 1-hexene up to 96%

at a temperature of 388 K and an ethylene pressure of 100 bar. In 2003, Chevron Phillips achieved industrial production of 1-hexene using this catalytic system.

With the increasing research on the ethylene trimerization reaction catalyzed by Cr catalysts, researchers have found many types of ligands, such as the PNP [163–165], SNS [166–168], NNN [169], PNS [170,171], and PN [172] types.

The PNP ligand is one of the most typical and important ligands for ethylene tri-/tetramerization. In 2002, Wass et al. [156] reported a series of PNP-type Cr complexes that can efficiently catalyze the ethylene trimerization reaction with commercially attractive production rates. The chromium complexes with ligands of the type  $\text{Ar}_2\text{PN}(\text{Me})\text{PAr}_2$  (Ar = ortho-substituted aryl group) were synthesized, which catalyze ethylene trimerization after MAO activation, and the  $\text{C}_6$  selectivity in the product was 81%, with 1-hexene accounting for 99.7%. Blann et al. [165] synthesized the PNP-type catalyst, which mainly produced 1-octene. However, when the H in the ortho position of the phenyl group was replaced by an ethyl group (Figure 19), the steric hindrance around the metal center caused by ortho ethyl substituents increased the selectivity of 1-hexene in the product, with the highest  $\text{C}_6$  product selectivity reaching 90.7% and 1-hexene accounting for 99.7% in the  $\text{C}_6$  product. Similarly, Kuhlmann et al. [173] connected a cyclohexyl group to the N atom of the PNP ligand. When both the ortho positions of the cyclohexane connected to the N atom were completely replaced by methyl groups, the product changed from  $\text{C}_8$ -dominant to a 1:1 mixture of 1-hexene and 1-octene. McGuinness et al. [174] showed that, when a dicyclohexylphosphine substitution was introduced at the phosphorus atom in the PNP ligand, the product was predominantly polyethylene (PE), and the catalytic activity was reduced. When the dicyclohexylphosphine substituent was replaced with diethylphosphine, the product was dominated by 1-hexene, with a selectivity of 99.2%.

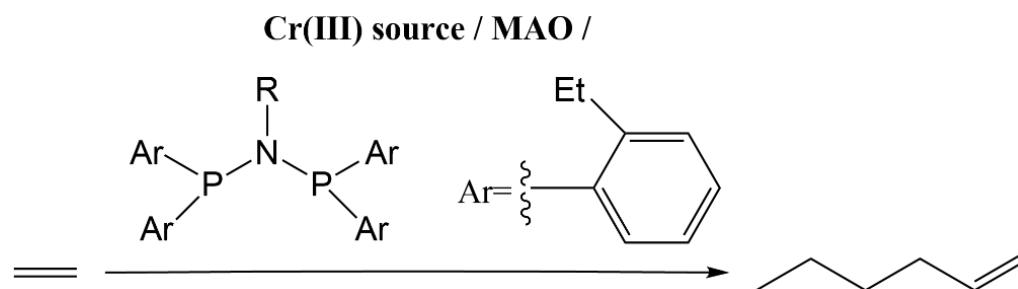


**Figure 19.** Cr-based catalysts with bulky diphosphinoamine ligands (complex 68). Reproduced from Ref. [165] with permission from the Royal Society of Chemistry.

Derivative species of PNP-type ligands (including SNS, PCCP, PNCN, etc.) can also be used in ethylene trimerization reactions. McGuinness et al. [174] researched SNS-type ligands as shown in Figure 20 for ethylene trimerization. After activation by the co-catalyst MAO, the SNS ligand also showed excellent ethylene trimerization ability, with TOF up to  $263,757 \text{ h}^{-1}$  and 1-hexene selectivity up to 97%. Temple et al. [166] synthesized SNS-type ligands with a catalytic activity of  $1.6 \times 10^5 \text{ g} \cdot \text{g}^{-1}_{\text{Cr}} \cdot \text{h}^{-1}$  after MAO activation, for which 98.4%  $\text{C}_6$  (including 99.8% 1-hexene) selectivity was achieved.

Boelter et al. [175] synthesized a series of PCCP-type ligands as shown in Figure 21 and found that the size of the phosphorus heterocyclopentane substituent affects the selectivity of the catalysts. With larger substituents, the proportion of 1-hexene in the product increases. Alam et al. [176] researched ethylene trimerization based on chromium(III) silylated diphosphinoamines. When the ligand skeleton in the system was  $\text{PSiNP}$ , the catalytic activity reached  $43,461 \text{ g} \cdot \text{g}^{-1}_{\text{Cr}} \cdot \text{h}^{-1}$ , with a selectivity of 83% for 1- $\text{C}_8$  and only 16% for 1- $\text{C}_6$ . When the catalyst ligand skeleton was  $\text{PSiNSiP}$ , the catalytic activity decreased to  $456 \text{ g} \cdot \text{g}^{-1}_{\text{Cr}} \cdot \text{h}^{-1}$ , but the selectivity for 1- $\text{C}_6$  increased to 91%. The authors believe that the steric hindrance of the metal active center and the angle of  $\text{P}-\text{Cr}-\text{P}$  affect the catalytic activity and selectivity of the catalyst. Zhang [177] also believes that, as the bond length becomes shorter, the ligand bite angle becomes smaller, and the catalytic activity increases.

Sydora et al. [157] synthesized a class of PNCN ligands that exhibit high catalytic activity for selective ethylene oligomerization. The molar ratio of 1-hexene to 1-octene in the product could be adjusted from 140 to 1.5 by adjusting the steric hindrance. As the steric hindrance increased, the catalyst activity decreased from  $54,700 \text{ kg}\cdot\text{g}^{-1}\text{Cr}\cdot\text{h}^{-1}$  to  $35,170 \text{ kg}\cdot\text{g}^{-1}\text{Cr}\cdot\text{h}^{-1}$ , and the selectivity of the  $\text{C}_6$  product also decreased from 93.6% to 52.2%, with 33.7%  $\text{C}_8$  and 4% PE present in the product. The rate of  $\alpha$ -olefin yield in the oligomers also decreased, and the proportion of  $\alpha$ - $\text{C}_6$  decreased from 99% to 45%. Radcliffe et al. [178] synthesized a PCN ligand that can selectively catalyze ethylene trimerization. By changing the substituents on the same ligand skeleton, high catalytic activity (Act. =  $2799 \text{ kg}\cdot\text{g}^{-1}\text{Cr}\cdot\text{h}^{-1}$ , 1- $\text{C}_6$  = 84%) or high product selectivity (Act. =  $797 \text{ kg}\cdot\text{g}^{-1}\text{Cr}\cdot\text{h}^{-1}$ , 1- $\text{C}_6$  = 97%) can be achieved. The ethylene trimerization using PNP-type ligands to produce 1-hexene will not be elaborated on here; it was discussed in detail by Uwe Rosenthal [179] in 2020.

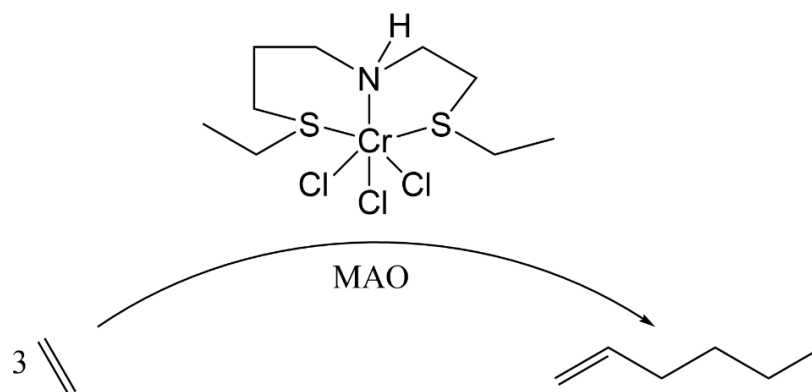


**Figure 20.** The structure of SNS-type ligand (complex 69). Reproduced with permission from Ref. [174]. Copyright 2005, American Chemical Society.

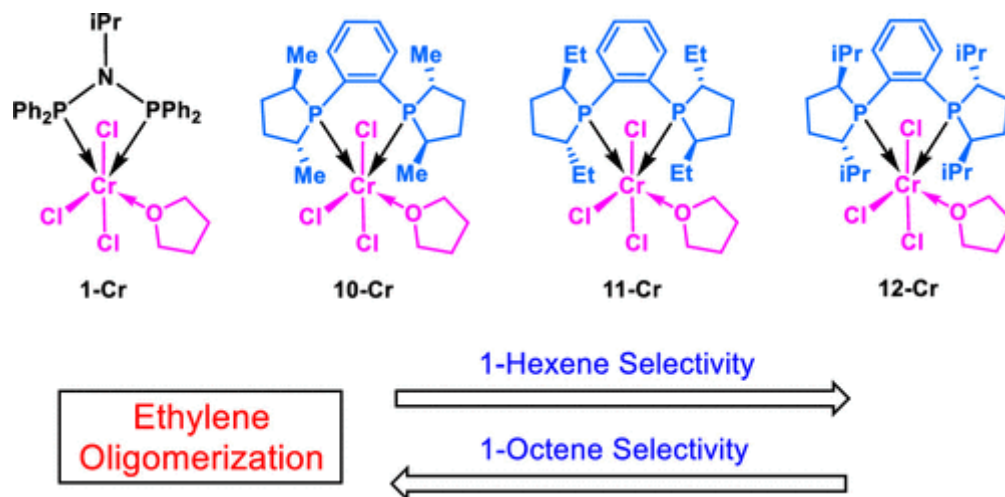


**Figure 21.** PCCP-type ligand structures with different substituents (from left to right: complexes 70–73). Reproduced with permission from Ref. [175]. Copyright 2020, American Chemical Society.

In the process of ethylene oligomerization catalyzed by Cr-based catalysts, it is inevitable to produce polyethylene, which will block the pipeline. Many research works suggest that PNP ligands can be induced by alkyl aluminum co-catalysts to form PPN ligands during catalytic reactions [180], which have high activity for ethylene polymerization reaction. Zhao et al. [181] synthesized PCCP-type ligands containing para-alkyl substituents with good results in ethylene trimerization and selectivity to PE below 0.1 wt%. The authors also found that the reactivity will be higher as the  $\sigma$ -donor ability of the ligand increases. The catalytic activity could reach up to  $5243 \text{ kg}\cdot\text{g}^{-1}\text{Cr}\cdot\text{h}^{-1}$ , while the selectivity for 1-hexene reached 74.9%.

Temperature and pressure also influence the reaction results. The optimal operating temperature for the catalysts synthesized by McGuinness [174] was in the range of 80–100 °C. At lower temperatures, activity decreases and leads to high polymer content, while, at higher temperatures, catalyst deactivation is observed and oligomers with higher carbon numbers form. Zhang et al. [163] synthesized PNP(NR<sub>2</sub>)<sub>2</sub>-containing catalysts and investigated the effects of temperature and pressure. When the pressure was 1 MPa, the catalytic activity and selectivity became volcanic with the increase in temperature, and the catalytic activity reached the highest at 318 K and the selectivity for C<sub>6</sub> products reached 92.23%, of which the proportion of 1-hexene was 98.87%. An increase in pressure can increase the reaction activity while reducing the selectivity towards C<sub>6</sub>. Soheili et al. [167] prepared SNS ligands in which the products varied greatly under different conditions. At a pressure of 15 bar, the reactivity reached 6420 g<sub>1-C6</sub>·g<sup>-1</sup><sub>Cr</sub>·h<sup>-1</sup>. However, when the pressure increased to 27 bar, the product was predominantly PE and the reactivity increased to 101,282 g<sub>PE</sub>·g<sup>-1</sup><sub>Cr</sub>·h<sup>-1</sup>.

The addition of co-catalysts had a similar effect on the reaction results. Choi et al. [182] synthesized chromium catalysts in situ with trifluoromethyl-containing ligands. When all the other conditions were equal, the proportional mixture of DMAO and TIBA as an activator was more catalytically active, more selective for 1-hexene, and only trace amounts of PE were produced when DMAO was used alone as an activator. The catalytic system achieved an activity value of 1248 g·mol<sup>-1</sup><sub>Cr</sub>·h<sup>-1</sup> with a high percentage (98.5 wt%) of 1-hexene in the product. The catalytic activity of the novel dendritic PNP chromium complexes synthesized by Wang et al. [183] showed a volcanic shape with the amount of co-catalyst MAO. The highest catalyst activity was achieved at Al/Cr = 700. Stennett [184] synthesized a dinuclear PNP-type ligand with higher activity and selectivity using AlMe<sub>3</sub> rather than MAO as a co-catalyst. The addition of excess MAO during the catalytic process leads to the production of a large amount of PE in the product.

Currently, there are also many researchers who have been combining computational chemistry and experimental science to study and design Cr-based catalyst ligands [185–187]. Fan et al. [185] combined Density Functional Theory (DFT) and Artificial Neural Networks (ANNs) to aid the design of new PNP ligands and successfully predict their performance. The authors also proposed that the spatial site resistance property affects the performance more significantly than the electronic property. Using DFT theory, Zhong et al. [186] investigated Cr/PCCP-type catalysts and concluded that the semi-instability of methoxy in the PCCP ligand is important for the selective regulation of ethylene trimerization. Similarly, Wang et al. [187], using DFT theory to study PCCP ligands, suggested that the coordination of the oxygen atom of the methoxy to the chromium center may be a key factor in the highly selective formation of 1-hexene.

In summary, different ligand backbones have significant effects on the reaction performance, and changing the backbone structure may lead to catalyst deactivation. The electronic effects and spatial site resistance of different substituents linked to the ligand backbone play a key role in catalyzing the selective oligomerization of ethylene, affecting both the catalytic activity and selectivity. Meanwhile, temperature, pressure, solvent, and co-catalysts are also the main factors affecting catalytic performance. In current research works, more and more researchers are using a combination of computational and experimental methods to study the catalytic reactions, which can help to find suitable catalysts efficiently and predict the catalytic behavior.

### 5.1.2. Ethylene Tetramerization

At the same time as the development of ethylene trimerization technology, many researchers explored the selective tetramerization of ethylene to produce 1-octene through Cr-based catalysts. Some researchers [188] remain skeptical about this. According to the metallacycle mechanism, obtaining 1-octene products through ethylene oligomerization requires the expansion of metal coordination compound intermediates from a seven-membered to a nine-membered metallacycle. However, in 2004, Bollmann et al. [189] of

SAAOL first reported the aluminum-oxide-activated  $\text{Cr}/(\text{R}_2)_2\text{P})_2\text{NR}_1$  system, where  $\text{R}_1$  and  $\text{R}_2$  are different substituents (Me, Ph, *i*-pr, etc.). The complex produces 1-octene with up to 70% selectivity while also producing small amounts of 1-hexene, methylcyclopentane, and methylene cyclopentane as the main byproducts. The results indicate that changing the steric hindrance and substituent type of ligands can affect the activity and selectivity of the catalyst. The catalyst ligands for ethylene tetramerization can be divided into PNP, PNPO, PNPN, PCP, and other ligands. These above ligands have been discussed in detail by Hao [13] and will not be repeated here.

### 5.1.3. Unselective Ethylene Oligomerization

The main products, 1-hexene or 1-octene, can be obtained using the above chromium catalysts in the catalytic ethylene oligomerization reaction, and the product distributions can be altered by changing the spatial site resistance of their active center. There are also some catalysts that are not capable of selective catalysis. Most Cr complexes with NNN- [190–192], NNO- [193,194], NO- [195,196], and NN-type [197,198] ligands exhibit high catalytic activity for ethylene oligomerization and provide a wide distribution of oligomer products from  $\text{C}_4$  to  $\text{C}_{24}$ .

Zhang et al. [190] synthesized NNN-type ligands as shown in Figure 22, after activation by MMAO, which exhibit high activity in ethylene oligomerization (up to  $7.36 \times 10^6 \text{ g}\cdot\text{mol}^{-1}\text{Cr}\cdot\text{h}^{-1}$ ), and the selectivity of  $\text{C}_4$ ,  $\text{C}_6$ , and  $\text{C}_8^+$  in the product is 19.3%, 32.8%, and 47.9%, respectively. Meanwhile, the catalyst also possesses high ethylene polymerization activity (up to  $1.28 \times 10^6 \text{ g}\cdot\text{mol}^{-1}\text{Cr}\cdot\text{h}^{-1}$ ). Milani et al. [199] synthesized Cr complexes with bidentate thioether-imine [N, S] ligands to catalyze ethylene oligomerization. The product range is very wide, with the highest selectivity of oligomers reaching 98.8%, and the selectivity of the ( $\text{C}_6$  and  $\text{C}_8$ ) products is 35.9%. However, when the reaction temperature decreased, the selectivity of the PE in the product reached 68.1%.

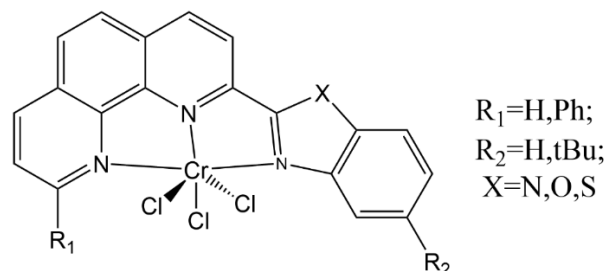


**Figure 22.** The structure of Cr(III) complexes bearing 2-benzazole-1,10-phenanthrolines (complex 74). Reproduced from Ref. [190] with permission from the Royal Society of Chemistry.

Generally speaking, as the temperature increases, the activity of ethylene oligomerization increases, but the selectivity of  $\alpha$ -olefins in the products decreases due to the accelerated rate of the chain isomerization reaction. However, when the temperature exceeds a certain range, the activity will decrease, which is due to the decomposition of active substances leading to catalyst deactivation or a decrease in the solubility of ethylene in the solvent at high temperatures. Relatively, the proportion of polymerization products decreases because the  $\beta$ -elimination reaction rate accelerates with increasing temperature. As the pressure increases, the catalytic activity increases and the proportion of long-chain products increases. The structures of ligands, co-catalysts [200], substituents [201], and the chemical environment all have a significant impact on the reaction activity.

## 5.2. Chromium-Based Heterogeneous Catalysts

Although homogeneous catalysts have high activity and good product selectivity, they are prone to deactivation. In contrast, heterogeneous catalysts can not only be separated from the product but also protect the active center of the catalyst. Cr-based heterogeneous

catalysts, such as immobilizing homogeneous catalysts onto supports [202,203], dispersing them into ionic liquids [204,205], and Cr-MOFs [206,207], were reported recently.

Lamb et al. [202] immobilized a Cr-based complex on oxides including  $\text{SiO}_2$ ,  $\gamma\text{-Al}_2\text{O}_3$ , and mixed  $\text{SiO}_2\text{-Al}_2\text{O}_3$  to obtain supported catalysts, which can perform selective ethylene trimerization after treatment via an aluminum activator. When using  $\text{SiO}_2$  or  $\text{SiO}_2\text{-Al}_2\text{O}_3$  as the carrier, high reaction activity and moderate trimerization selectivity can be achieved, while, when using  $\gamma\text{-Al}_2\text{O}_3$  as the carrier, the reaction activity decreases significantly, and the product is mainly PE.

Gao et al. [205] introduced organoaluminum-based ionic liquids in the PNP/Cr/MAO system and above 98% selectivity for (1-hexene and 1-octene) was obtained. The separation of the catalyst from the product can be achieved by decanting the upper organic phase containing the product, and the catalyst can be reused by adding a new solvent and MAO. The catalytic activity gradually decreased in three cycles because small amounts of impurities were inevitably introduced during the circulation process, but the selectivity for 1-hexene was still above 96%.

Fallahi et al. [203] immobilized SNS ligands onto ionic liquid-functionalized SBA-15 for ethylene trimerization. Under optimal conditions, the catalytic activity can reach  $19,394 \text{ g}_{1\text{-C}_6} \text{ g}_{\text{Cr}}^{-1} \text{ h}^{-1}$ , and the selectivity for 1-hexene can reach 99.7%. Müller et al. [204] dissolved the homogeneous catalyst Cr-PNP in hydrogenated dibenzyltoluene (H18-DBT) together with the co-catalyst MAO and then dispersed the solution onto activated carbon or SiC. This catalyst can be used in continuous gas-phase reactions for up to 220 h. After 40 h of reaction, the selectivity of the product tends to stabilize, with a selectivity of 25.2% for 1-hexene and 44.6% for 1-octene. However, PE, which is continuously produced during the reaction, adheres to the catalyst surface affecting the contact between the ethylene and the active center, leading to deactivation.

Goetjen et al. [206] synthesized Cr-SIM-NU-1000 via solvothermal deposition in MOFs (SIM), and the ethylene conversion rate can reach 20% at 1 bar of ethylene partial pressure and ambient temperature. It is worth noting that the amount of cocatalyst used in the reaction was very low ( $\text{Al/Cr} = 3$ ), and the reaction raw material was a mixture of  $\text{H}_2$  and  $\text{C}_2\text{H}_4$  to suppress the production of polymers. However, the distribution of the products in this catalytic system was very broad, with  $\text{C}_8\text{-C}_{18}$  accounting for 79%. Liu et al. [207] selected MIL-100(Cr) for selective ethylene oligomerization because it can eliminate two water molecules connected to the metal sites after vacuum heating and form coordinatively unsaturated metal sites for reaction. Different pre-treatment temperatures can cause a change in the valence state of Cr, which leads to a transition from ethylene oligomerization to polymerization.

## 6. Other Metals-Based Heterogeneous Catalysts

In addition to the nickel, iron, cobalt, and chromium metals that have been explored in the heterogeneous ethylene oligomerization reaction, other metals (such as Ru, Zr, and Ga) have been successively applied for this reaction in recent years with promising catalytic performance.

Iker Agirrezabal-Telleria et al. [208] developed a method for tailoring (Ru)HKUST-1 defects via thermal-based protocols. Thermal defect engineering leads to (Ru)HKUST-1, with the defective nodes exhibiting a well-defined active site for ethylene dimerization. In the absence of solvents and co-catalysts, the catalysts can achieve activities up to  $\text{TOF} = 200 \text{ h}^{-1}$ , stable catalytic times in excess of 120 h, and selectivity of 99% for 1-butene. At the same time, the authors demonstrated that the behavior of the active Ru-H sites produced by an economical and versatile thermal method is the same as that of the active Ru-H sites prepared by conventional ligand engineering methods.

Nicole J. LiBretto et al. [209] reported that silica-supported single-site catalysts containing fixed main group  $\text{Zn}^{2+}$  or  $\text{Ga}^{3+}$  ionic sites catalyze the ethylene oligomerization reaction to reach an equilibrium distribution of linear olefins at rates similar to those of  $\text{Ni}^{2+}$  (Table 3). By varying the spatial velocity of  $\text{C}_2\text{H}_4$ , at a conversion of 3%, the selectivity

of Ga/SiO<sub>2</sub> for butene was 75.9%, for hexene was 16.8%, and for octene was 6.4% at 1 atm and 250 °C. Moreover, Zn/SiO<sub>2</sub> showed 85.5% selectivity for butene, 2% for hexene, and no 1-octene products. Both catalysts were able to catalyze stably for at least more than 25 h under the above conditions. At low conversion (3%), Ga/SiO<sub>2</sub> is more favorable for the generation of high-carbon olefins compared to the Zn/SiO<sub>2</sub> and Ni/SiO<sub>2</sub> catalysts. The product distribution of Ga/SiO<sub>2</sub> does not change significantly, whereas the transfer of the products of Zn/SiO<sub>2</sub> to lower carbon numbers can be achieved at high pressure: 30.6 atm with high conversions. The authors also demonstrated that the catalytic cycle begins with the heterodissociation of the vinyl C–H bond of ethylene, and the reaction intermediates and basic steps were shown to be consistent with the Cossee–Arlman mechanism for Ni<sup>2+</sup> transition metal catalysts.

**Table 3.** Product selectivity and conversion for ethylene oligomerization at 250 °C.

Catalyst	Pressure (atm)	Conversion (%) <sup>1</sup>	Selectivity (%)				Rate (mol C <sub>4</sub> H <sub>8</sub> molM <sup>-1</sup> s <sup>-1</sup> ) <sup>2</sup>
			Butenes (C <sub>4</sub> =)	Hexenes (C <sub>6</sub> =)	Octenes (C <sub>8</sub> =)	C <sub>10</sub> +	
Ni/SiO <sub>2</sub>	1	3	86.1	11.8	0.4	0	15 × 10 <sup>-4</sup>
Ga/SiO <sub>2</sub>		3	75.9	16.8	6.4	0	7 × 10 <sup>-4</sup>
Zn/SiO <sub>2</sub>		3	85.5	2.0	0.0	0	1 × 10 <sup>-4</sup>
Ni/SiO <sub>2</sub>	30.6	20.7	86.2	11.1	2.9	0	7 × 10 <sup>-2</sup>
Ga/SiO <sub>2</sub>		20.6	74.2	16.1	4.9	4.2	8 × 10 <sup>-2</sup>
Zn/SiO <sub>2</sub>		15.2	96.0	0.8	0	0	5 × 10 <sup>-2</sup>

<sup>1</sup> Conversion was varied using different space velocities over 1 g of catalyst in a 3/8 in diameter quartz reactor tube. <sup>2</sup> Rate was calculated by normalizing the mol C<sub>4</sub>H<sub>8</sub>/s produced by the total mol of metal on the catalyst (rate = (mol C<sub>4</sub>H<sub>8</sub>)/(mol M \* s)).

## 7. Summary and Outlook

In this article, we summarize the progress of ethylene oligomerization in homogeneous and heterogeneous phases using different metals (Ni, Fe, Co, Cr, etc.) as active sites. In the homogeneous catalytic system, we mainly discuss the effects of the molecular structure, electronic, and coordination states of complexes on their catalytic activity and selectivity. In heterogeneous catalytic systems, we mainly concentrate on the influence of various supports (metal–organic frameworks, covalent organic frameworks, molecular sieves, etc.) and different ways to introduce active centers regarding the activity in ethylene oligomerization.

Due to the discovery of the “nickel effect”, nickel, as a post-transition metal, was first used in the ethylene oligomerization reaction. In recent decades, researchers have made significant progress in this field. Firstly, the “SHOP” ethylene oligomerization process derived from the neutral [P, O] ligand catalytic system reached a total olefin production of 1.3 million tons/year in 2018 [2,210]. Secondly, the invention of  $\alpha$ -diimine ligands has made nickel-based catalysts designable and enabled the study of the influence of spatial site resistance and electronic effects on catalytic performance [22]. Finally, the development of single-site MOF catalysts bridges the gap between homogeneous and heterogeneous catalysis and provides an ideal platform for elucidating structure–activity relationships using molecular chemistry mechanisms in combination with computational chemistry, transient spectroscopy, and advanced diffraction techniques. For homogeneous systems, the choice of the nickel precursor and the design of ligands naturally play tremendous roles regarding the catalytic effect. In summary, nickel catalysts for the dimerization of ethylene are monocentric asymmetric complexes of Ni<sup>II</sup> with tridentate ligands containing two or three nitrogen atoms in the conjugated system. The development of new catalytic systems continues to be based on a trial-and-error approach. Although high selectivity can be achieved with homogeneous catalysts, it is poorly recoverable; on the other hand, heterogeneous catalysts are robust but lack selectivity. Among the heterogeneous nickel catalysts mentioned above, metal–organic frameworks are very attractive supports due to their high porosity and site density, unlimited variety of designs, and possible post-synthesis modifications. Ni-ZIF-8 (0.4 wt%), Ni(1%)-MFU-4l, and MIL-125(Ti)-NH<sub>2</sub>(Ni) employ

Ni as a catalytic active site and present higher activity and selectivity towards 1-butene. However, some challenges remain for MOFs in olefin oligomerization reactions. On the one hand, secondary reactions such as isomerization and dimerization hinder the generation of  $\alpha$ -olefins and linear selectivity, which must be avoided using rationally designed MOF catalysts. On the other hand, the catalyst deactivation due to the accumulation of polymers on the active sites was addressed by rationally selecting and designing the building blocks of MOFs, adjusting the pore size of MOFs, introducing flexible substituents around the active centers, and increasing the percentage of surface active sites.

The discovery of highly active iron and cobalt catalysts is another milestone in the development of olefin oligomerization catalysts using late transition metals. The linearities of the oligomerization products obtained using iron and cobalt catalysts in homogeneous systems are higher compared to nickel-based catalysts. Schiff base ligands exhibit interesting and diverse coordination chemistry and have therefore attracted much attention in the design of catalysts for ethylene oligomerization [211,212]. This ligand and its derivatives can form N–metal bonds via the coordination of nitrogen atoms into monodentate or multi-dentate. In addition, it can act as a donor and acceptor in hydrogen bonding interactions. Carbocyclic fused N,N,N-iron complexes show real industrial promise with the successful use of an imino-phe naphtholine–iron complex for the production of  $\alpha$ -olefins in a 500-ton pilot plant managed by Sinopec in China. In homogeneous catalyzed reactions, iron and cobalt catalysts, although less active than nickel catalysts, have greater selectivity towards higher-carbon products (1-hexene and 1-octene). In heterogeneous catalytic reactions, fewer types of iron and cobalt catalysts have been developed, such as MIL-100(Fe) and carbon-supported cobalt catalysts. Uncontrollable exotherms leading to rapid catalyst deactivation and low activity are problems that need to be solved for the development of heterogeneous iron and cobalt catalysts.

Chromium-based catalysts, as pre-transition metals, have highly electron-deficient properties, are extremely sensitive to water–oxygen, and require large amounts of the expensive co-catalyst MAO for activation, which have led to their limitation in the production of linear  $\alpha$ -olefins by ethylene oligomerization. However, these catalysts have become a hot topic in recent years due to their ability to selectively produce high-carbon linear olefins. For chromium-based catalysts, the most commonly used ligands for ethylene trimerization/tetramerization are PNP and the alternative diphosphine ligands PNNP, PCP, PCCP, and PCNCP [213–216]. When the catalyst contains P- and N-electron-donating multidentate ligands, it has a high selectivity potential for the production of 1-hexene and 1-octene [170]. The reactivity of chromium catalysts in heterogeneous reactions is still not comparable to that of post-transition metal catalysts.

In addition, catalysts based on zinc [209], gallium [209], and ruthenium [208] metals are continuously being developed for the heterogeneous catalytic reaction of ethylene oligomerization. The exploration of these catalysts not only extends the types of active metals in the field but also contributes to the understanding of the mechanism of the oligomerization process.

Although there has been extensive research using various metals-based catalysts for ethylene oligomerization, there are still some issues to be solved. First, most catalysts use a large amount of co-catalyst during the catalytic process, but their prices are relatively expensive and their applied conditions are often harsh (without O<sub>2</sub> and H<sub>2</sub>O). Finding cheaper and easily operated co-catalysts or modifying the existing co-catalysts has become an important issue. Second, heterogeneous catalysts have the advantages of being easily separated from the products and being recyclable. Compared with homogeneous catalysis, heterogeneous catalysis is more promising for industrial applications, but most of the current heterogeneous catalysts are less active for ethylene oligomerization and less selective for linear  $\alpha$ -olefins than homogeneous catalysts. Except SHOP, other industrialized approaches to ethylene oligomerization based on heterogeneous catalysis have not yet been realized. There remains a significant need to optimize heterogeneous catalysts compared to the currently industrialized homogeneous methods, particularly in terms of

improving product selectivity. Third, the demand for high-performance polymerization materials prepared using high-carbon  $\alpha$ -olefins (1-hexene and 1-octene) is increasing, so the development of catalysts for the efficient production of high-carbon  $\alpha$ -olefins is urgent. In addition to changing the reaction conditions (pressure, temperature, amount of co-catalyst, etc.), the development of new metal-based catalysts and new ligands may be a promising solution. Furthermore, the similarities between homogeneous and heterogeneous catalysis may be utilized to gain more insight into the selectivity control mechanism. Finally, despite the general acceptance of the Cossee–Arlman mechanism and metallacyclic mechanism for ethylene oligomerization, there is a lack of in situ real-time evidence. Finding a completely new method or technique might break this bottleneck in the study of these mechanisms. In conclusion, the development of highly selective  $\alpha$ -olefin formation processes remains a major challenge for academia and industry.

**Author Contributions:** A.P. and Z.H. collected the data, writing—original draft. G.L.: writing—review and editing, Supervision. All authors have read and agreed to the published version of the manuscript.

**Funding:** This research received no external funding.

**Data Availability Statement:** Data are contained within the article.

**Conflicts of Interest:** The authors declare no conflicts of interest.

## Appendix A

It is necessary to make notes regarding the presentation of the results of the catalytic tests in the review:

(1) There are two types of catalyst activity calculations; one is  $[g_{\text{product}} \times g_{\text{catalyst}}^{-1} \times h^{-1}]$  and the other is  $[g_{\text{product}} \times \text{mol}_M^{-1} \times h^{-1}]$ , expressed as Equations (A1) and (A2), respectively (M is metal).

$$[\text{Activity}] = \frac{\text{ethylene oligomerization products (g)}}{\text{catalyst(g)} \times \text{reaction time (h)}} = [g_{\text{product}} \times g_{\text{catalyst}}^{-1} \times h^{-1}] \quad (\text{A1})$$

$$[\text{Activity}] = \frac{\text{ethylene oligomerization products (g)}}{\text{metal molecular (mol)} \times \text{reaction time (h)}} = [g_{\text{product}} \times \text{mol}_M^{-1} \times h^{-1}] \quad (\text{A2})$$

(2) In the experiments, TOF  $[\text{mol}_{\text{C}_2\text{H}_4} \times \text{mol}_M^{-1} \times h^{-1}]$  is calculated using Equation (A3) (M is metal):

$$[\text{TOF}] = \frac{\text{Activity} [g \times \text{mol}_M^{-1} \times h^{-1}]}{\text{Mr}_{\text{C}_2\text{H}_4} [g \times \text{mol}^{-1}]} = [h^{-1}] \quad (\text{A3})$$

## References

1. Speiser, F.; Braunstein, P.; Saussine, L. New Nickel Ethylene Oligomerization Catalysts Bearing Bidentate P,N-Phosphinopyridine Ligands with Different Substituents  $\alpha$  to Phosphorus. *Organometallics* **2004**, *23*, 2625–2632. [[CrossRef](#)]
2. Breuil, P.A.R.; Magna, L.; Olivier-Bourbigou, H. Role of Homogeneous Catalysis in Oligomerization of Olefins: Focus on Selected Examples Based on Group 4 to Group 10 Transition Metal Complexes. *Catal. Lett.* **2015**, *145*, 173–192. [[CrossRef](#)]
3. de Klerk, A. Thermal cracking of Fischer-Tropsch waxes. *Ind. Eng. Chem. Res.* **2007**, *46*, 5516–5521. [[CrossRef](#)]
4. Li, C.; Ying, W.; Cao, F.; Zhang, H.; Fang, D. Effects of Impregnation Solvents on Catalytic Performance of Co-Ru-ZrO<sub>2</sub>/ $\gamma$ -Al<sub>2</sub>O<sub>3</sub> Catalyst for Fischer-Tropsch Synthesis. *Pet. Sci. Technol.* **2008**, *26*, 704–716. [[CrossRef](#)]
5. Liu, X.H.; Linghu, W.S.; Li, X.H.; Asami, K.; Fujimoto, K. Effects of solvent on Fischer-Tropsch synthesis. *Appl. Catal. A Gen.* **2006**, *303*, 251–257. [[CrossRef](#)]
6. Cheng, Y.; Lin, J.; Wu, T.J.; Wang, H.; Xie, S.H.; Pei, Y.; Yan, S.R.; Qiao, M.H.; Zong, B.N. Mg and K dual-decorated Fe-on-reduced graphene oxide for selective catalyzing CO hydrogenation to light olefins with mitigated CO<sub>2</sub> emission and enhanced activity. *Appl. Catal. B Environ.* **2017**, *204*, 475–485. [[CrossRef](#)]
7. Li, A.L.; Tian, D.X.; Zhao, Z.B. DFT studies on the reaction mechanism for the selective oxidative dehydrogenation of light alkanes by BN catalysts. *N. J. Chem.* **2020**, *44*, 11584–11592. [[CrossRef](#)]

8. Wang, G.W.; Zhang, S.; Zhu, X.L.; Li, C.Y.; Shan, H.H. Dehydrogenation versus hydrogenolysis in the reaction of light alkanes over Ni-based catalysts. *J. Ind. Eng. Chem.* **2020**, *86*, 1–12. [[CrossRef](#)]
9. Yan, B.; Li, W.C.; Lu, A.H. Metal-free silicon boride catalyst for oxidative dehydrogenation of light alkanes to olefins with high selectivity and stability. *J. Catal.* **2019**, *369*, 296–301. [[CrossRef](#)]
10. Rajapaksha, R.; Samanta, P.; Quadrelli, E.A.; Canivet, J. Heterogenization of molecular catalysts within porous solids: The case of Ni-catalyzed ethylene oligomerization from zeolites to metal-organic frameworks. *Chem. Soc. Rev.* **2023**, *52*, 8059–8076. [[CrossRef](#)]
11. Wang, M.Z.; Wu, W.; Wang, X.; Huang, X.; Nai, Y.N.; Wei, X.Y.; Mao, G.L. Research progress of iron-based catalysts for selective oligomerization of ethylene. *RSC Adv.* **2020**, *10*, 43640–43652. [[CrossRef](#)] [[PubMed](#)]
12. Wang, Z.; Solan, G.A.; Zhang, W.J.; Sun, W.H. Carbocyclic-fused N,N,N-pincer ligands as ring-strain adjustable supports for iron and cobalt catalysts in ethylene oligo-/polymerization. *Coord. Chem. Rev.* **2018**, *363*, 92–108. [[CrossRef](#)]
13. Hao, B.B.; Alam, F.; Jiang, Y.; Wang, L.B.; Fan, H.A.; Ma, J.; Chen, Y.H.; Wang, Y.T.; Jiang, T. Selective ethylene tetramerization: An overview. *Inorg. Chem. Front.* **2023**, *10*, 2860–2902. [[CrossRef](#)]
14. Keim, W. Oligomerization of Ethylene to  $\alpha$ -Olefins: Discovery and Development of the Shell Higher Olefin Process (SHOP). *Angew. Chem.-Int. Ed.* **2013**, *52*, 12492–12496. [[CrossRef](#)] [[PubMed](#)]
15. McGuinness, D.S. Olefin Oligomerization via Metallacycles: Dimerization, Trimerization, Tetramerization, and Beyond. *Chem. Rev.* **2011**, *111*, 2321–2341. [[CrossRef](#)] [[PubMed](#)]
16. Cossee, P. On the mechanism of cis-ligand insertion. *Recl. Trav. Chim. Pays-Bas* **1966**, *85*, 1151–1160. [[CrossRef](#)]
17. Arlman, E.J.; Cossee, P. Ziegler-Natta catalysis III. Stereospecific polymerization of propene with the catalyst system  $\text{TiCl}_3\text{-AlEt}_3$ . *J. Catal.* **1964**, *3*, 99–104. [[CrossRef](#)]
18. Briggs, J.R. The selective trimerization of ethylene to hex-1-ene. *J. Chem. Soc.-Chem. Commun.* **1989**, 674–675. [[CrossRef](#)]
19. Chhabra, S.; Smith, D.M.; Bell, N.L.; Watson, A.J.B.; Bühl, M.; Cole-Hamilton, D.J.; Bode, B.E. First experimental evidence for a bis-ethene chromium(I) complex forming from an activated ethene oligomerization catalyst. *Sci. Adv.* **2020**, *6*, eabd7057. [[CrossRef](#)]
20. Fischer, K.; Jonas, K.; Misbach, P.; Stabba, R.; Wilke, G. The “Nickel Effect” *Angew. Chem. Int. Ed. Engl.* **1973**, *12*, 943–953. [[CrossRef](#)]
21. Peuckert, M.; Keim, W. A new nickel complex for the oligomerization of ethylene. *Organometallics* **1983**, *2*, 594–597. [[CrossRef](#)]
22. Johnson, L.K.; Killian, C.M.; Brookhart, M. New Pd(II)- and Ni(II)-Based Catalysts for Polymerization of Ethylene and  $\alpha$ -Olefins. *J. Am. Chem. Soc.* **1995**, *117*, 6414–6415. [[CrossRef](#)]
23. Tuskaev, V.A.; Gagieva, S.C.; Kurmaev, D.A.; Zvukova, T.M.; Fedyanin, I.V.; Bulychev, B.M. Synthesis, characterization and ethylene oligomerization behavior of new nickel(II) octafluoro- $\alpha$ -diimine complex. *Inorg. Chim. Acta* **2016**, *442*, 167–171. [[CrossRef](#)]
24. Rishina, L.A.; Kissin, Y.V.; Lalayan, S.S.; Gagieva, S.C.; Kurmaev, D.A.; Tuskaev, V.A.; Bulychev, B.M. New  $\alpha$ -diimine nickel complexes-Synthesis and catalysis of alkene oligomerization reactions. *J. Mol. Catal. A Chem.* **2016**, *423*, 495–502. [[CrossRef](#)]
25. Liu, J.; Wang, J.; Chen, L.; Zhang, N.; Lan, T.; Wang, L. Ethylene Oligomerization Study Bearing Nickel (II) and Cobalt (II) Complexes with N, O-Donor Schiff Bases as Ligands. *Chemistryselect* **2019**, *4*, 13959–13963. [[CrossRef](#)]
26. Falivene, L.; Wiedemann, T.; Goettker-Schnetmann, I.; Caporaso, L.; Cavallo, L.; Mecking, S. Control of Chain Walking by Weak Neighboring Group Interactions in Unsymmetrical Catalysts. *J. Am. Chem. Soc.* **2018**, *140*, 1305–1312. [[CrossRef](#)]
27. Wang, K.; Gao, R.; Hao, X.; Sun, W.-H. Nickel complexes bearing 2-(1H-benzo[d]imidazol-2-yl)-N-benzylidenequinolin-8-amine: Synthesis, structure and catalytic ethylene oligomerization. *Catal. Commun.* **2009**, *10*, 1730–1733. [[CrossRef](#)]
28. Zhao, W.; Qian, Y.L.; Huang, J.L.; Duan, J.J. Novel neutral arylnickel(II) phosphine catalysts containing 2-oxazolinyphenolato N-O chelate ligands for ethylene oligomerization and propylene dimerization. *J. Organomet. Chem.* **2004**, *689*, 2614–2623. [[CrossRef](#)]
29. Wang, C.; Friedrich, S.; Younkin, T.R.; Li, R.T.; Grubbs, R.H.; Bansleben, D.A.; Day, M.W. Neutral Nickel(II)-Based Catalysts for Ethylene Polymerization. *Organometallics* **1998**, *17*, 3149–3151. [[CrossRef](#)]
30. Zhang, S.; Pattacini, R.; Jie, S.; Braunstein, P. A phosphino-oxazoline ligand as a P,N-bridge in palladium/cobalt or P,N-chelate in nickel complexes: Catalytic ethylene oligomerization. *Dalton Trans.* **2012**, *41*, 379–386. [[CrossRef](#)]
31. Ortiz de la Tabla, L.; Matas, I.; Palma, P.; Álvarez, E.; Cámpora, J. Nickel and Palladium Complexes with New Phosphinito-Imine Ligands and Their Application as Ethylene Oligomerization Catalysts. *Organometallics* **2012**, *31*, 1006–1016. [[CrossRef](#)]
32. Zhang, S.; Pattacini, R.; Braunstein, P. Reactions of a Phosphinoimino-thiazoline-Based Metalloligand with Organic and Inorganic Electrophiles and Metal-Induced Ligand Rearrangements. *Organometallics* **2010**, *29*, 6660–6667. [[CrossRef](#)]
33. Boulens, P.; Lutz, M.; Jeanneau, E.; Olivier-Bourbigou, H.; Reek, J.N.H.; Breuil, P.-A.R. Iminobisphosphines to (Non-)Symmetrical Diphosphinoamine Ligands: Metal-Induced Synthesis of Diphosphorus Nickel Complexes and Application in Ethylene Oligomerization Reactions. *Eur. J. Inorg. Chem.* **2014**, *2014*, 3754–3762. [[CrossRef](#)]
34. Song, K.; Gao, H.; Liu, F.; Pan, J.; Guo, L.; Zai, S.; Wu, Q. Syntheses, Structures, and Catalytic Ethylene Oligomerization Behaviors of Bis(phosphanyl)aminenickel(II) Complexes Containing N-Functionalized Pendant Groups. *Eur. J. Inorg. Chem.* **2009**, *2009*, 3016–3024. [[CrossRef](#)]
35. Cooley, N.A.; Green, S.M.; Wass, D.F.; Heslop, K.; Orpen, A.G.; Pringle, P.G. Nickel Ethylene Polymerization Catalysts Based on Phosphorus Ligands. *Organometallics* **2001**, *20*, 4769–4771. [[CrossRef](#)]

36. Ghisolfi, A.; Fliedel, C.; Rosa, V.; Monakhov, K.Y.; Braunstein, P. Combined Experimental and Theoretical Study of Bis(diphenylphosphino)(N-thioether)amine-Type Ligands in Nickel(II) Complexes for Catalytic Ethylene Oligomerization. *Organometallics* **2014**, *33*, 2523–2534. [[CrossRef](#)]
37. Tayade, K.N.; Mane, M.V.; Sen, S.; Murthy, C.N.; Tembe, G.L.; Pillai, S.M.; Vanka, K.; Mukherjee, S. A catalytic and DFT study of selective ethylene oligomerization by nickel(II) oxime-based complexes. *J. Mol. Catal. A Chem.* **2013**, *366*, 238–246. [[CrossRef](#)]
38. Xiao, L.; Zhang, M.; Gao, R.; Cao, X.; Sun, W.-H. 2-(1H-2-Benzimidazolyl)-6-(1-(arylimino)ethyl)pyridylnickel Complexes: Synthesis, Characterization, and Ethylene Oligomerization. *Aust. J. Chem.* **2010**, *63*, 109–115. [[CrossRef](#)]
39. Yang, Y.; Yang, P.; Zhang, C.; Li, G.; Yang, X.-J.; Wu, B.; Janiak, C. Synthesis, structure, and catalytic ethylene oligomerization of nickel complexes bearing 2-pyrazolyl substituted 1,10-phenanthroline ligands. *J. Mol. Catal. A Chem.* **2008**, *296*, 9–17. [[CrossRef](#)]
40. Jie, S.; Zhang, S.; Sun, W.-H. 2-arylimino-9-phenyl-1,10-phenanthroline-iron, -cobalt and -nickel complexes: Synthesis, characterization and ethylene oligomerization behavior. *Eur. J. Inorg. Chem.* **2007**, *2007*, 5584–5598. [[CrossRef](#)]
41. Zhang, W.; Wang, Y.; Yu, J.; Redshaw, C.; Hao, X.; Sun, W.-H. 2-(N-Alkylcarboxamide)-6-iminopyridyl palladium and nickel complexes: Coordination chemistry and catalysis. *Dalton Trans.* **2011**, *40*, 12856–12865. [[CrossRef](#)]
42. Chen, Y.; Hao, P.; Zuo, W.; Gao, K.; Sun, W.-H. 2-(1-Isopropyl-2-benzimidazolyl)-6-(1-aryliminoethyl)pyridyl transition metal (Fe, Co, and Ni) dichlorides: Syntheses, characterizations and their catalytic behaviors toward ethylene reactivity. *J. Organomet. Chem.* **2008**, *693*, 1829–1840. [[CrossRef](#)]
43. Zhang, J.; Liu, S.; Li, A.; Ye, H.; Li, Z. Nickel(II) complexes chelated by 2,6-pyridinedicarboxamide: Syntheses, characterization, and ethylene oligomerization. *N. J. Chem.* **2016**, *40*, 7027–7033. [[CrossRef](#)]
44. Ulbrich, A.H.D.P.S.; Bergamo, A.L.; Casagrande, O.D.L., Jr. Oligomerization of ethylene using tridentate nickel catalysts bearing ether-pyrazol ligands with pendant O- and S-donor groups. *Catal. Commun.* **2011**, *16*, 245–249. [[CrossRef](#)]
45. Bekmukhamedov, G.E.; Sukhov, A.V.; Kuchkaev, A.M.; Yakhvarov, D.G. Ni-Based Complexes in Selective Ethylene Oligomerization Processes. *Catalysts* **2020**, *10*, 498. [[CrossRef](#)]
46. Olivier-Bourbigou, H.; Breuil, P.A.R.; Magna, L.; Michel, T.; Pastor, M.F.E.; Delcroix, D. Nickel Catalyzed Olefin Oligomerization and Dimerization. *Chem. Rev.* **2020**, *120*, 7919–7983. [[CrossRef](#)]
47. Crabtree, R.H. Deactivation in Homogeneous Transition Metal Catalysis: Causes, Avoidance, and Cure. *Chem. Rev.* **2015**, *115*, 127–150. [[CrossRef](#)]
48. Ockwig, N.W.; Delgado-Friedrichs, O.; O’Keeffe, M.; Yaghi, O.M. Reticular chemistry: Occurrence and taxonomy of nets and grammar for the design of frameworks. *Acc. Chem. Res.* **2005**, *38*, 176–182. [[CrossRef](#)]
49. Liu, J.; Ye, J.; Li, Z.; Otake, K.-I.; Liao, Y.; Peters, A.W.; Noh, H.; Truhlar, D.G.; Gagliardi, L.; Cramer, C.J.; et al. Beyond the Active Site: Tuning the Activity and Selectivity of a Metal-Organic Framework-Supported Ni Catalyst for Ethylene Dimerization. *J. Am. Chem. Soc.* **2018**, *140*, 11174–11178. [[CrossRef](#)]
50. Britovsek, G.J.P.; Bruce, M.; Gibson, V.C.; Kimberley, B.S.; Maddox, P.J.; Mastroianni, S.; McTavish, S.J.; Redshaw, C.; Solan, G.A.; Strömberg, S.; et al. Iron and cobalt ethylene polymerization catalysts bearing 2,6-bis(imino)pyridyl ligands: Synthesis, structures, and polymerization studies. *J. Am. Chem. Soc.* **1999**, *121*, 8728–8740. [[CrossRef](#)]
51. Small, B.L.; Brookhart, M.; Bennett, A.M.A. Highly Active Iron and Cobalt Catalysts for the Polymerization of Ethylene. *J. Am. Chem. Soc.* **1998**, *120*, 4049–4050. [[CrossRef](#)]
52. Zhang, C.-L.; Zhou, T.; Li, Y.-Q.; Lu, X.; Guan, Y.-B.; Cao, Y.-C.; Cao, G.-P. Microenvironment Modulation of Metal-Organic Frameworks (MOFs) for Coordination Olefin Oligomerization and (co)Polymerization. *Small* **2023**, *19*, 2205898. [[CrossRef](#)] [[PubMed](#)]
53. Chen, C.; Alalouni, M.R.; Dong, X.; Cao, Z.; Cheng, Q.; Zheng, L.; Meng, L.; Guan, C.; Liu, L.; Abou-Hamad, E.; et al. Highly Active Heterogeneous Catalyst for Ethylene Dimerization Prepared by Selectively Doping Ni on the Surface of a Zeolitic Imidazolate Framework. *J. Am. Chem. Soc.* **2021**, *143*, 7144–7153. [[CrossRef](#)] [[PubMed](#)]
54. Chen, L.; Jiang, Y.; Huo, H.; Liu, J.; Li, Y.; Li, C.; Zhang, N.; Wang, J. Metal-organic framework-based composite Ni@MOF as Heterogeneous catalyst for ethylene trimerization. *Appl. Catal. A Gen.* **2020**, *594*, 117457. [[CrossRef](#)]
55. Yeh, B.; Vicchio, S.P.; Chheda, S.; Zheng, J.; Schmid, J.; Löbber, L.; Bermejo-Deval, R.; Gutiérrez, O.Y.; Lercher, J.A.; Lu, C.C.; et al. Site Densities, Rates, and Mechanism of Stable Ni/UiO-66 Ethylene Oligomerization Catalysts. *J. Am. Chem. Soc.* **2021**, *143*, 20274–20280. [[CrossRef](#)] [[PubMed](#)]
56. Komurcu, M.; Lazzarini, A.; Kaur, G.; Borfecchia, E.; Oien-Odegaard, S.; Gianolio, D.; Bordiga, S.; Lillerud, K.P.; Olsbye, U. Co-catalyst free ethene dimerization over Zr-based metal-organic framework (UiO-67) functionalized with Ni and bipyridine. *Catal. Today* **2021**, *369*, 193–202. [[CrossRef](#)]
57. Sharma, R.K.; Yadav, P.; Yadav, M.; Gupta, R.; Rana, P.; Srivastava, A.; Zboril, R.; Varma, R.S.; Antonietti, M.; Gawande, M.B. Recent development of covalent organic frameworks (COFs): Synthesis and catalytic (organic-electro-photo) applications. *Mater. Horiz.* **2020**, *7*, 411–454. [[CrossRef](#)]
58. Rozhko, E.; Bavykina, A.; Osadchii, D.; Makkee, M.; Gascon, J. Covalent organic frameworks as supports for a molecular Ni based ethylene oligomerization catalyst for the synthesis of long chain olefins. *J. Catal.* **2017**, *345*, 270–280. [[CrossRef](#)]
59. Li, D.; Guo, L.; Li, F.; Huang, J.; Li, J.; Li, M.; Li, C. Synthesis and catalytic behavior of nickel heterogenized in covalent organic frameworks as precatalysts in ethylene oligomerization. *Microporous Mesoporous Mater.* **2022**, *338*, 111979. [[CrossRef](#)]
60. Guo, L.; Gao, Y.; Huang, J.; Xue, J.; Li, F.; Li, C. Imine-linked covalent organic frameworks coordinated with nickel for ethylene oligomerization. *J. Appl. Polym. Sci.* **2023**, *140*, e53320. [[CrossRef](#)]

61. Lallemand, M.; Rusu, O.A.; Dumitriu, E.; Finiels, A.; Fajula, F.; Hulea, V. NiMCM-36 and NiMCM-22 catalysts for the ethylene oligomerization: Effect of zeolite texture and nickel cations/acid sites ratio. *Appl. Catal. A Gen.* **2008**, *338*, 37–43. [[CrossRef](#)]
62. Andrei, R.D.; Popa, M.L.; Fajula, F.; Hulea, V. Heterogeneous oligomerization of ethylene over highly active and stable Ni-ALSBA-15 mesoporous catalysts. *J. Catal.* **2015**, *323*, 76–84. [[CrossRef](#)]
63. Shin, D.Y.; Yoon, J.H.; Baik, H.; Lee, S.J. A way to avoid polymeric side products during the liquid-phase ethylene oligomerization with SBA-15 supported (bpy)Ni(II)Cl<sub>2</sub> heterogeneous catalyst. *Appl. Catal. A Gen.* **2020**, *590*, 117363. [[CrossRef](#)]
64. Lacarriere, A.; Robin, J.; Swierczynski, D.; Finiels, A.; Fajula, F.; Luck, F.; Hulea, V. Distillate-Range Products from Non-Oil-Based Sources by Catalytic Cascade Reactions. *ChemSuschem* **2012**, *5*, 1787–1792. [[CrossRef](#)] [[PubMed](#)]
65. Mohamed, H.O.; Parsapur, R.K.; Hita, I.; Ramirez, A.; Huang, K.-W.; Gascon, J.; Castano, P. Stable and reusable hierarchical ZSM-5 zeolite with superior performance for olefin oligomerization when partially coked. *Appl. Catal. B Environ.* **2022**, *316*, 121582. [[CrossRef](#)]
66. Mohamed, H.O.; Velisoju, V.K.; Hita, I.; Abed, O.; Parsapur, R.K.; Zambrano, N.; Ben Hassine, M.; Morlanes, N.; Emwas, A.-H.; Huang, K.-W.; et al. Highly productive framework bounded Ni<sup>2+</sup> on hierarchical zeolite for ethylene oligomerization. *Chem. Eng. J.* **2023**, *475*, 146077. [[CrossRef](#)]
67. McCaig, J.; Lamb, H.H. Ni-H-Beta Catalysts for Ethylene Oligomerization: Impact of Parent Cation on Ni Loading, Speciation, and Siting. *Catalysts* **2022**, *12*, 824. [[CrossRef](#)]
68. Seufitelli, G.V.S.; Park, J.J.W.; Tran, P.N.; Dichiaro, A.; Resende, F.L.P.; Gustafson, R. The Role of Nickel and Bronsted Sites on Ethylene Oligomerization with Ni-H-Beta Catalysts. *Catalysts* **2022**, *12*, 565. [[CrossRef](#)]
69. Lee, M.; Yoon, J.W.; Kim, Y.; Yoon, J.S.; Chae, H.-J.; Han, Y.-H.; Hwang, D.W. Ni/SIRAL-30 as a heterogeneous catalyst for ethylene oligomerization. *Appl. Catal. A Gen.* **2018**, *562*, 87–93. [[CrossRef](#)]
70. Hu, Y.; Zhang, Y.; Han, Y.; Sheng, D.; Shan, D.; Liu, X.; Cheng, A. Ultrathin Nickel-Based Metal–Organic Framework Nanosheets as Reusable Heterogeneous Catalyst for Ethylene Dimerization. *ACS Appl. Nano Mater.* **2019**, *2*, 136–142. [[CrossRef](#)]
71. Arrozi, U.S.F.; Bon, V.; Kutzscher, C.; Senkovska, I.; Kaskel, S. Towards highly active and stable nickel-based metal-organic frameworks as ethylene oligomerization catalysts. *Dalton Trans.* **2019**, *48*, 3415–3421. [[CrossRef](#)]
72. Wang, C.; Li, G.; Guo, H. Heterogeneous dimerization of ethylene by coordinatively unsaturated metal sites in two forms of Ni-MIL-77. *Mol. Catal.* **2022**, *524*, 112340. [[CrossRef](#)]
73. Chen, C.L.; Alalouni, M.R.; Xiao, P.Y.; Li, G.X.; Pan, T.T.; Shen, J.; Cheng, Q.P.; Dong, X.L. Ni-Loaded 2D Zeolitic Imidazolate Framework as a Heterogeneous Catalyst with Highly Activity for Ethylene Dimerization. *Ind. Eng. Chem. Res.* **2022**, *61*, 14374–14381. [[CrossRef](#)]
74. Metzger, E.D.; Brozek, C.K.; Comito, R.J.; Dincă, M. Selective Dimerization of Ethylene to 1-Butene with a Porous Catalyst. *ACS Cent. Sci.* **2016**, *2*, 148–153. [[CrossRef](#)]
75. Metzger, E.D.; Comito, R.J.; Wu, Z.; Zhang, G.; Dubey, R.C.; Xu, W.; Miller, J.T.; Dinca, M. Highly Selective Heterogeneous Ethylene Dimerization with a Scalable and Chemically Robust MOF Catalyst. *ACS Sustain. Chem. Eng.* **2019**, *7*, 6654–6661. [[CrossRef](#)]
76. Chen, C.L.; Meng, L.K.; Alalouni, M.R.; Dong, X.L.; Wu, Z.P.; Zuo, S.W.; Zhang, H.B. Ultra-Highly Active Ni-Doped MOF-5 Heterogeneous Catalysts for Ethylene Dimerization. *Small* **2023**, *19*, e2301235. [[CrossRef](#)]
77. Li, Z.; Schweitzer, N.M.; League, A.B.; Bernaldes, V.; Peters, A.W.; Getsoian, A.B.; Wang, T.C.; Miller, J.T.; Vjunov, A.; Fulton, J.L.; et al. Sintering-Resistant Single-Site Nickel Catalyst Supported by Metal Organic Framework. *J. Am. Chem. Soc.* **2016**, *138*, 1977–1982. [[CrossRef](#)]
78. Canivet, J.; Aguado, S.; Schuurman, Y.; Farrusseng, D. MOF-Supported Selective Ethylene Dimerization Single-Site Catalysts through One-Pot Postsynthetic Modification. *J. Am. Chem. Soc.* **2013**, *135*, 4195–4198. [[CrossRef](#)]
79. Liu, B.; Jie, S.; Bu, Z.; Li, B.-G. Postsynthetic modification of mixed-linker metal-organic frameworks for ethylene oligomerization. *RSC Adv.* **2014**, *4*, 62343–62346. [[CrossRef](#)]
80. Madrahimov, S.T.; Gallagher, J.R.; Zhang, G.; Meinhart, Z.; Garibay, S.J.; Delferro, M.; Miller, J.T.; Farha, O.K.; Hupp, J.T.; Nguyen, S.T. Gas-Phase Dimerization of Ethylene under Mild Conditions Catalyzed by MOF Materials Containing (bpy)Ni<sup>II</sup> Complexes. *ACS Catal.* **2015**, *5*, 6713–6718. [[CrossRef](#)]
81. Kyogoku, K.; Yamada, C.; Suzuki, Y.; Nishiyama, S.; Fukumoto, K.; Yamamoto, H.; Indo, S.; Sano, M.; Miyake, T. Syntheses of Metal-organic Framework Compounds Containing Ni-bipyridyl Complex for Oligomerization of Ethylene. *J. Jpn. Pet. Inst.* **2010**, *53*, 308–312. [[CrossRef](#)]
82. Gonzalez, M.I.; Oktawiec, J.; Long, J.R. Ethylene oligomerization in metal-organic frameworks bearing nickel(II) 2,2'-bipyridine complexes. *Faraday Discuss.* **2017**, *201*, 351–367. [[CrossRef](#)]
83. Arrozi, U.S.F.; Bon, V.; Krause, S.; Lübken, T.; Weiss, M.S.; Senkovska, I.; Kaskel, S. In Situ Imine-Based Linker Formation for the Synthesis of Zirconium MOFs: A Route to CO<sub>2</sub> Capture Materials and Ethylene Oligomerization Catalysts. *Inorg. Chem.* **2020**, *59*, 350–359. [[CrossRef](#)]
84. Alshehri, S.M.; Ahamad, T.; Aldalbahi, A.; Alhokbany, N. Pyridylimine Cobalt(II) and Nickel(II) Complex Functionalized Multiwalled Carbon Nanotubes and Their Catalytic Activities for Ethylene Oligomerization. *Adv. Polym. Technol.* **2016**, *35*, 21528–21538. [[CrossRef](#)]

85. Kohler, F.T.U.; Gaertner, K.; Hager, V.; Haumann, M.; Sternberg, M.; Wang, X.; Szesni, N.; Meyer, K.; Wasserscheid, P. Dimerization of ethene in a fluidized bed reactor using Ni-based Supported Ionic Liquid Phase (SILP) catalysts. *Catal. Sci. Technol.* **2014**, *4*, 936–947. [[CrossRef](#)]
86. Aid, A.; Andrei, R.D.; Amokrane, S.; Cammarano, C.; Nibou, D.; Hulea, V. Ni-exchanged cationic clays as novel heterogeneous catalysts for selective ethylene oligomerization. *Appl. Clay Sci.* **2017**, *146*, 432–438. [[CrossRef](#)]
87. Kim, M.J.; Ahn, S.; Yi, J.; Hupp, J.T.; Notestein, J.M.; Farha, O.K.; Lee, S.J. Ni(II) complex on a bispyridine-based porous organic polymer as a heterogeneous catalyst for ethylene oligomerization. *Catal. Sci. Technol.* **2017**, *7*, 4351–4354. [[CrossRef](#)]
88. Yoon, J.S.; Park, M.B.; Kim, Y.; Hwang, D.W.; Chae, H.-J. Effect of Metal Oxide-Support Interactions on Ethylene Oligomerization over Nickel Oxide/Silica-Alumina Catalysts. *Catalysts* **2019**, *9*, 933. [[CrossRef](#)]
89. Finiels, A.; Fajula, F.; Hulea, V. Nickel-based solid catalysts for ethylene oligomerization—A review. *Catal. Sci. Technol.* **2014**, *4*, 2412–2426. [[CrossRef](#)]
90. Small, B.L.; Brookhart, M. Iron-Based Catalysts with Exceptionally High Activities and Selectivities for Oligomerization of Ethylene to Linear  $\alpha$ -Olefins. *J. Am. Chem. Soc.* **1998**, *120*, 7143–7144. [[CrossRef](#)]
91. Gibson, V.C.; Redshaw, C.; Solan, G.A. Bis(imino)pyridines: Surprisingly reactive ligands and a gateway to new families of catalysts. *Chem. Rev.* **2007**, *107*, 1745–1776. [[CrossRef](#)]
92. Britovsek, G.J.P.; Gibson, V.C.; McTavish, S.J.; Solan, G.A.; White, A.J.P.; Williams, D.J.; Britovsek, G.J.P.; Kimberley, B.S.; Maddox, P.J. Novel olefin polymerization catalysts based on iron and cobalt. *Chem. Commun.* **1998**, 849–850. [[CrossRef](#)]
93. Ngcobo, M.; Nose, H.; Jayamani, A.; Ojwach, S.O. Structural and ethylene oligomerization studies of chelating (imino)phenol Fe(II), Co(II) and Ni(II) complexes: An experimental and theoretical approach. *N. J. Chem.* **2022**, *46*, 6219–6229. [[CrossRef](#)]
94. Guo, J.; Chen, Q.; Zhang, W.; Liang, T.; Sun, W.-H. The benzhydryl-modified 2-imino-1,10-phenanthrolyliron precatalyst in ethylene oligomerization. *J. Organomet. Chem.* **2021**, *936*, 121713. [[CrossRef](#)]
95. Sheng, D.; Zhang, Y.; Wang, Z.; Xu, G.; Song, Q.; Shan, D.; Hou, H. Selective ethylene oligomerization based on Fe-containing metal-organic coordination polymer catalysts. *J. Organomet. Chem.* **2021**, *956*, 122128. [[CrossRef](#)]
96. Malsakova, I.S.; Pervova, I.G.; Belov, G.P.; Khasbiullin, I.I.; Ivanova, N.A.; Frolova, E.N.; Lipunov, I.N. Synthesis, structure, and catalytic properties of iron complexes with mono- and bisformazans in sulfide oxidation and ethylene oligomerization reactions. *Pet. Chem.* **2015**, *55*, 217–223. [[CrossRef](#)]
97. Appukuttan, V.K.; Liu, Y.; Son, B.C.; Ha, C.-S.; Suh, H.; Kim, I. Iron and Cobalt Complexes of 2,3,7,8-Tetrahydroacridine-4,5(1H,6H)-diimine Sterically Modulated by Substituted Aryl Rings for the Selective Oligomerization to Polymerization of Ethylene. *Organometallics* **2011**, *30*, 2285–2294. [[CrossRef](#)]
98. Xiao, T.; Zhang, W.; Lai, J.; Sun, W.-H. Iron-oriented ethylene oligomerization and polymerization: The Iron Age or a flash in the pan. *C. R. Chim.* **2011**, *14*, 851–855. [[CrossRef](#)]
99. Tomov, A.K.; Gibson, V.C.; Britovsek, G.J.P.; Long, R.J.; van Meurs, M.; Jones, D.J.; Tellmann, K.P.; Chirinos, J.J. Distinguishing Chain Growth Mechanisms in Metal-catalyzed Olefin Oligomerization and Polymerization Systems: C<sub>2</sub>H<sub>4</sub>/C<sub>2</sub>D<sub>4</sub> Co-oligomerization/Polymerization Experiments Using Chromium, Iron, and Cobalt Catalysts. *Organometallics* **2009**, *28*, 7033–7040. [[CrossRef](#)]
100. Görl, C.; Beck, N.; Kleiber, K.; Alt, H.G. Iron(III) complexes with meta-substituted bis(arylimino)pyridine ligands: Catalyst precursors for the selective oligomerization of ethylene. *J. Mol. Catal. A Chem.* **2012**, *352*, 110–127. [[CrossRef](#)]
101. Li, G.; Ge, Y.; Xu, G.; Dai, S. The electronic effects on unsymmetrical Bis(imino)pyridyl iron(III) catalyzed ethylene polymerization. *J. Organomet. Chem.* **2020**, *923*, 121457. [[CrossRef](#)]
102. Görl, C.; Alt, H.G. Influence of the para-substitution in bis(arylimino)pyridine iron complexes on the catalytic oligomerization and polymerization of ethylene. *J. Organomet. Chem.* **2007**, *692*, 4580–4592. [[CrossRef](#)]
103. Kissin, Y.V.; Qian, C.; Xie, G.; Chen, Y. Multi-center nature of ethylene polymerization catalysts based on 2,6-bis(imino)pyridyl complexes of iron and cobalt. *J. Polym. Sci. Part A Polym. Chem.* **2006**, *44*, 6159–6170. [[CrossRef](#)]
104. Minaev, B.; Baryshnikova, A.; Sun, W.-H. Spin-dependent effects in ethylene polymerization with bis(imino)pyridine iron(II) complexes. *J. Organomet. Chem.* **2016**, *811*, 48–65. [[CrossRef](#)]
105. Cartes, M.Á.; Rodríguez-Delgado, A.; Palma, P.; Sánchez, L.J.; Cámpora, J. Direct evidence for a coordination–insertion mechanism of ethylene oligomerization catalysed by neutral 2,6-bisiminopyridine iron monoalkyl complexes. *Catal. Sci. Technol.* **2014**, *4*, 2504–2507. [[CrossRef](#)]
106. Li, H.-y.; Duan, B.-g.; Hu, Y.-l. The influence of substituent electronic effect on ethylene oligomerization activities of bis(imino)pyridyl Fe(II) catalysts: A combined molecular mechanics and charge equilibration method. *Chin. J. Polym. Sci.* **2009**, *27*, 711. [[CrossRef](#)]
107. Guo, C.Y.; Xu, H.; Zhang, M.G.; Zhang, X.H.; Yan, F.W.; Yuan, G.Q. Immobilization of bis(imino)pyridine iron complexes onto mesoporous molecular sieves and their catalytic performance in ethylene oligomerization. *Catal. Commun.* **2009**, *10*, 1467–1471. [[CrossRef](#)]
108. Ittel, S.D.; Johnson, L.K.; Brookhart, M. Late-Metal Catalysts for Ethylene Homo- and Copolymerization. *Chem. Rev.* **2000**, *100*, 1169–1204. [[CrossRef](#)] [[PubMed](#)]
109. Bariashir, C.; Zhang, Q.-Y.; Ulambayar, B.; Solan, G.A.; Liang, T.-L.; Sun, W.-H. High Temperature Iron Ethylene Polymerization Catalysts Bearing N, N, N'-2-(1-(2,4-Dibenzhydryl-6-fluorophenylimino)ethyl)-6-(1-(arylphenylimino)ethyl)pyridines. *Chin. J. Polym. Sci.* **2024**, *42*, 188–201. [[CrossRef](#)]

110. Zhao, W.; Yue, E.; Wang, X.; Yang, W.; Chen, Y.; Hao, X.; Cao, X.; Sun, W.-H. Activity and stability spontaneously enhanced toward ethylene polymerization by employing 2-(1-(2,4-dibenzhydrylnaphthylimino)ethyl)-6-(1-(arylimino)ethyl) pyridyliron(II) dichlorides. *J. Polym. Sci. Part A Polym. Chem.* **2017**, *55*, 988–996. [[CrossRef](#)]
111. Kaul, F.A.R.; Puchta, G.T.; Frey, G.D.; Herdtweck, E.; Herrmann, W.A. Iminopyridine Complexes of 3d Metals for Ethylene Polymerization: Comparative Structural Studies and Ligand Size Controlled Chain Termination. *Organometallics* **2007**, *26*, 988–999. [[CrossRef](#)]
112. Xie, G.; Li, T.; Zhang, A. Highly active and selective ethylene oligomerization catalysts: Asymmetric 2,6-bis(imino)pyridyl iron (II) complexes with alkyl and halogen substituents. *Inorg. Chem. Commun.* **2010**, *13*, 1199–1202. [[CrossRef](#)]
113. Bianchini, C.; Mantovani, G.; Meli, A.; Migliacci, F.; Zanobini, F.; Laschi, F.; Sommazzi, A. Oligomerisation of Ethylene to Linear  $\alpha$ -Olefins by new C<sub>s</sub>- and C<sub>1</sub>-Symmetric [2,6-Bis(imino)pyridyl]iron and -cobalt Dichloride Complexes. *Eur. J. Inorg. Chem.* **2003**, *2003*, 1620–1631. [[CrossRef](#)]
114. Sun, W.-H.; Xing, Q.; Yu, J.; Novikova, E.; Zhao, W.; Tang, X.; Liang, T.; Redshaw, C. Probing the Characteristics of Mono- or Bimetallic (Iron or Cobalt) Complexes Bearing 2,4-Bis(6-iminopyridin-2-yl)-3H-benzazepines: Synthesis, Characterization, and Ethylene Reactivity. *Organometallics* **2013**, *32*, 2309–2318. [[CrossRef](#)]
115. Zhang, N.; Wu, Y.; Li, Y.; Chen, L.; Zhang, M.; Wang, J. Star iminopyridyl iron, cobalt and nickel complexes: Synthesis, molecular structures, and evaluation as ethylene oligomerization catalysts. *Polym. Bull.* **2022**, *79*, 4219–4231. [[CrossRef](#)]
116. Zhang, N.; Wang, J.; Huo, H.; Chen, L.; Shi, W.; Li, C.; Wang, J. Iron, cobalt and nickel complexes bearing hyperbranched iminopyridyl ligands: Synthesis, characterization and evaluation as ethylene oligomerization catalysts. *Inorg. Chim. Acta* **2018**, *469*, 209–216. [[CrossRef](#)]
117. Li, C.-Q.; Wang, F.-F.; Gao, R.; Sun, P.; Zhang, N.; Wang, J. Bidentate iron complexes based on hyperbranched salicylaldimine ligands and their catalytic behavior toward ethylene oligomerization. *Transit. Met. Chem.* **2017**, *42*, 339–346. [[CrossRef](#)]
118. Nyamato, G.S.; Alam, M.G.; Ojwach, S.O.; Akerman, M.P. (Pyrazolyl)-(phosphinoyl)pyridine iron(II), cobalt(II) and nickel(II) complexes: Synthesis, characterization and ethylene oligomerization studies. *J. Organomet. Chem.* **2015**, *783*, 64–72. [[CrossRef](#)]
119. Rossetto, E.; Nicola, B.P.; de Souza, R.F.; Bernardo-Gusmão, K.; Pergher, S.B.C. Heterogeneous complexes of nickel MCM-41 with  $\beta$ -diimine ligands: Applications in olefin oligomerization. *J. Catal.* **2015**, *323*, 45–54. [[CrossRef](#)]
120. Kim, I.; Han, B.H.; Kim, J.S.; Ha, C.-S. Bis(imino)pyridyl Co(II) and Fe(II) catalysts immobilized on SBA-15 mesoporous material: New highly active supported catalysts for the polymerization of ethylene. *Catal. Lett.* **2005**, *101*, 249–253. [[CrossRef](#)]
121. Ionkin, A.S.; Marshall, W.J.; Adelman, D.J.; Bobik Fones, B.; Fish, B.M.; Schiffhauer, M.F.; Spence, R.E.; Xie, T. High-Temperature Catalysts for the Production of  $\alpha$ -Olefins Based on Iron(II) and Cobalt(II) Tridentate Bis(imino)pyridine Complexes with a Double Pattern of Substitution: *o*-Methyl plus *o*-Fluorine in the Same Imino Arm. *Organometallics* **2008**, *27*, 1147–1156. [[CrossRef](#)]
122. Ionkin, A.S.; Marshall, W.J.; Adelman, D.J.; Fones, B.B.; Fish, B.M.; Schiffhauer, M.F. High-Temperature Catalysts for the Production of  $\alpha$ -Olefins Based on Iron(II) and Iron(III) Tridentate Bis(imino)pyridine Complexes with Double Pattern of Substitution: *ortho*-Methyl plus *meta*-Aryl. *Organometallics* **2006**, *25*, 2978–2992. [[CrossRef](#)]
123. Zheng, Z.; Liu, J.; Li, Y. Ethylene polymerization with silica-supported bis(imino)pyridyl iron(II) catalysts. *J. Catal.* **2005**, *234*, 101–110. [[CrossRef](#)]
124. Guo, C.-Y.; Xu, H.; Zhang, M.; Yang, H.-J.; Yan, F.; Yuan, G. Copolymerization of ethylene and in situ-generated  $\alpha$ -olefins to high-performance linear low-density polyethylene with a two-catalyst system supported on mesoporous molecular sieves. *Polym. Int.* **2010**, *59*, 725–732. [[CrossRef](#)]
125. Jayamani, A.; Nyamato, G.S.; Ojwach, S.O. Ethylene oligomerization reactions catalyzed by homogeneous and silica immobilized NO Fe(II) and Co(II) complexes. *J. Organomet. Chem.* **2019**, *903*, 120987. [[CrossRef](#)]
126. Armspach, D.; Matt, D.; Peruch, F.; Lutz, P. Cyclodextrin-Encapsulated Iron Catalysts for the Polymerization of Ethylene. *Eur. J. Inorg. Chem.* **2003**, *2003*, 805–809. [[CrossRef](#)]
127. Bouilhac, C.; Cloutet, E.; Cramail, H.; Deffieux, A.; Taton, D. Functionalized Star-Like Polystyrenes as Organic Supports of a Tridentate Bis(imino)pyridyliron/Aluminic Derivative Catalytic System for Ethylene Polymerization. *Macromol. Rapid Commun.* **2005**, *26*, 1619–1625. [[CrossRef](#)]
128. Han, Y.; Zhang, Y.; Zhang, Y.L.; Cheng, A.C.; Hu, Y.P.; Wang, Z.H. Selective ethylene tetramerization with iron-based metal-organic framework MIL-100 to obtain C<sub>8</sub> alkanes. *Appl. Catal. A Gen.* **2018**, *564*, 183–189. [[CrossRef](#)]
129. Kaul, F.A.R.; Puchta, G.T.; Schneider, H.; Bielert, F.; Mihailos, D.; Herrmann, W.A. Immobilization of bis(imino)pyridyliron(II) complexes on silica. *Organometallics* **2002**, *21*, 74–82. [[CrossRef](#)]
130. Ngcobo, M.; Ouissa, A.; Kleist, W.; Thiel, W.R.; Ojwach, S.O. Regulating the physical properties of silica immobilized Fe(II), Ni(II) and Co(II) catalysts towards ethylene oligomerization reactions. *Mol. Catal.* **2023**, *549*, 113465. [[CrossRef](#)]
131. Ngcobo, M.; Ojwach, S.O. Ethylene oligomerization reactions catalyzed by recyclable Fe(II), Ni(II) and Co(II) complexes immobilized on Fe<sub>3</sub>O<sub>4</sub> magnetic nanoparticles. *Mol. Catal.* **2021**, *508*, 111583. [[CrossRef](#)]
132. Ba, J.; Du, S.; Yue, E.; Hu, X.; Flisak, Z.; Sun, W.-H. Constrained formation of 2-(1-(arylimino)ethyl)-7-arylimino-6,6-dimethylcyclopentapyridines and their cobalt(II) chloride complexes: Synthesis, characterization and ethylene polymerization. *RSC Adv.* **2015**, *5*, 32720–32729. [[CrossRef](#)]
133. Huang, Y.; Zhang, R.; Liang, T.; Hu, X.; Solan, G.A.; Sun, W.-H. Selectivity Effects on N,N,N'-Cobalt Catalyzed Ethylene Dimerization/Trimerization Dictated through Choice of Aluminoxane Cocatalyst. *Organometallics* **2019**, *38*, 1143–1150. [[CrossRef](#)]

134. Guo, J.; Zhang, W.; Liang, T.; Sun, W.-H. Revisiting the 2-imino-1,10-phenanthrolylmetal precatalyst in ethylene oligomerization: Benzhydryl-modified cobalt(II) complexes and their dimerization of ethylene. *Polyhedron* **2021**, *193*, 114865. [[CrossRef](#)]
135. Antonov, A.A.; Semikolenova, N.V.; Talsi, E.P.; Bryliakov, K.P. Catalytic ethylene oligomerization on cobalt(II) bis(imino)pyridine complexes bearing electron-withdrawing groups. *J. Organomet. Chem.* **2019**, *884*, 55–58. [[CrossRef](#)]
136. Caovilla, M.; Thiele, D.; de Souza, R.F.; Gregorio, J.R.; Bernardo-Gusmao, K. Cobalt- $\beta$ -diimine complexes for ethylene oligomerization. *Catal. Commun.* **2017**, *101*, 85–88. [[CrossRef](#)]
137. Chen, L.; Ma, L.; Jiang, Y.; Liu, J.; Li, C.; Zhang, N.; Wang, J. Synthesis and characterization of iron, cobalt and nickel complexes bearing para-phenylene-linked pyridine imine ligand and their catalytic properties for ethylene oligomerization. *Polym. Bull.* **2021**, *78*, 415–432. [[CrossRef](#)]
138. Khoshsefat, M.; Ahmadjo, S.; Zohuri, G.H.; Ma, Y.; Sun, W.-H. From tetramerization to oligomerization/polymerization of ethylene by dinuclear pyridyl-imine Co- and Ni-based catalysts. *Appl. Organomet. Chem.* **2023**, *37*, e7226. [[CrossRef](#)]
139. Wei, W.; Yu, B.; Alam, F.; Huang, Y.; Cheng, S.; Jiang, T. Cobalt(II)-based ethylene dimerization catalysts with silicon-bridged diphosphine ligands. *Appl. Organomet. Chem.* **2018**, *32*, e4604. [[CrossRef](#)]
140. Zhang, L.; Meng, X.J.; Chen, Y.H.; Cao, C.G.; Jiang, T. Chromium-Based Ethylene Tetramerization Catalysts Supported by Silicon-Bridged Diphosphine Ligands: Further Combination of High Activity and Selectivity. *Chemcatchem* **2017**, *9*, 76–79. [[CrossRef](#)]
141. Härzschel, S.; Kühn, F.E.; Wöhl, A.; Müller, W.; Al-Hazmi, M.H.; Alqahtani, A.M.; Müller, B.H.; Peulecke, N.; Rosenthal, U. Comparative study of new chromium-based catalysts for the selective tri- and tetramerization of ethylene. *Catal. Sci. Technol.* **2015**, *5*, 1678–1682. [[CrossRef](#)]
142. Wang, J.; Li, H.-Y.; Song, L.; Shi, W.-G.; Zhang, N.; Li, C.-Q. Cobalt complexes based on dendritic PAMAM bridged salicylaldimine ligands: Synthesis, characterization and performance in ethylene oligomerization. *J. Macromol. Sci. Part A Pure Appl. Chem.* **2016**, *53*, 709–715. [[CrossRef](#)]
143. Li, C.; Wang, F.; Lin, Z.; Zhang, N.; Wang, J. Cobalt complexes based on hyperbranched salicylaldimine ligands as catalyst precursors for ethylene oligomerization. *Appl. Organomet. Chem.* **2017**, *31*, e3756. [[CrossRef](#)]
144. Zhang, N.; Wang, S.-h.; Song, L.; Li, C.-q.; Wang, J. Hyperbranched macromolecules bridged salicylaldimine cobalt complexes: Synthesis, characterization and ethylene oligomerization studies. *Chem. Pap.* **2017**, *71*, 1037–1046. [[CrossRef](#)]
145. Ngcobo, M.; Nyamato, G.S.; Ojwach, S.O. Structural elucidation of N<sup>o</sup>O (ethylimino-methyl)phenol Fe(II) and Co(II) complexes and their applications in ethylene oligomerization catalysis. *Mol. Catal.* **2019**, *478*, 110590. [[CrossRef](#)]
146. Zubkevich, S.V.; Tuskaev, V.A.; Gagieva, S.C.; Kayda, A.S.; Khrustalev, V.N.; Pavlov, A.A.; Zarubin, D.N.; Bulychev, B.M. NNO-Heteroscorpionate nickel (II) and cobalt (II) complexes for ethylene oligomerization: The unprecedented formation of odd carbon number olefins. *Appl. Organomet. Chem.* **2020**, *34*, e5873. [[CrossRef](#)]
147. Xu, Z.; Zhao, D.; Chada, J.P.; Rosenfeld, D.C.; Rogers, J.L.; Hermans, L.; Huber, G.W. Olefin conversion on nitrogen-doped carbon-supported cobalt catalyst: Effect of feedstock. *J. Catal.* **2017**, *354*, 213–222. [[CrossRef](#)]
148. Xu, Z.; Chada, J.P.; Xu, L.; Zhao, D.; Rosenfeld, D.C.; Rogers, J.L.; Hermans, L.; Mavrikakis, M.; Huber, G.W. Ethylene Dimerization and Oligomerization to 1-Butene and Higher Olefins with Chromium-Promoted Cobalt on Carbon Catalyst. *ACS Catal.* **2018**, *8*, 2488–2497. [[CrossRef](#)]
149. Jonathan, A.; Eagan, N.M.; Bruns, D.L.; Stahl, S.S.; Lanci, M.P.; Dumesic, J.A.; Huber, G.W. Ethylene oligomerization into linear olefins over cobalt oxide on carbon catalyst. *Catal. Sci. Technol.* **2021**, *11*, 3599–3608. [[CrossRef](#)]
150. Jonathan, A.; Tomashek, E.G.; Lanci, M.P.; Dumesic, J.A.; Huber, G.W. Reaction kinetics study of ethylene oligomerization into linear olefins over carbon-supported cobalt catalysts. *J. Catal.* **2021**, *404*, 954–963. [[CrossRef](#)]
151. Jonathan, A.; Dastidar, R.G.; Wang, C.; Dumesic, J.A.; Huber, G.W. Effect of catalyst support on cobalt catalysts for ethylene oligomerization into linear olefins. *Catal. Sci. Technol.* **2022**, *12*, 3639–3649. [[CrossRef](#)]
152. Zhu, K.; An, Y.; Yu, F.; Liu, L.; Zhong, L. Structure-Performance Evolution of Cobalt-Ammonia Activated Carbon Catalyst for Ethylene Oligomerization. *Catal. Lett.* **2022**, *152*, 2131–2140. [[CrossRef](#)]
153. Tang, J.; Zhang, N.; Shi, D.; Zhang, F.; Tang, J. Synthesis of UiO-66-NH<sub>2</sub> Grafted Pyridineimine Cobalt Catalyst and Its Catalytic Performance in Ethylene Oligomerization. *Chin. J. Appl. Chem.* **2022**, *39*, 258–265. [[CrossRef](#)]
154. Weng, Z.; Teo, S.; Hor, T.S.A. Chromium(III) catalysed ethylene tetramerization promoted by bis(phosphino)amines with an N-functionalized pendant. *Dalton Trans.* **2007**, 3493–3498. [[CrossRef](#)]
155. Mao, G.; Ning, Y.; Hu, W.; Li, S.; Song, X.; Niu, B.; Jiang, T. Synthesis of a novel triple-site diphosphinoamine (PNP) ligand and its applications in ethylene tetramerization. *Chin. Sci. Bull.* **2008**, *53*, 3511–3515. [[CrossRef](#)]
156. Carter, A.; Cohen, S.A.; Cooley, N.A.; Murphy, A.; Scutt, J.; Wass, D.F. High activity ethylene trimerisation catalysts based on diphosphine ligands. *Chem. Commun.* **2002**, 858–859. [[CrossRef](#)]
157. Sydora, O.L.; Jones, T.C.; Small, B.L.; Nett, A.J.; Fischer, A.A.; Carney, M.J. Selective Ethylene Tri-/Tetramerization Catalysts. *ACS Catal.* **2012**, *2*, 2452–2455. [[CrossRef](#)]
158. Zhang, J.; Braunstein, P.; Hor, T.S.A. Highly Selective Chromium(III) Ethylene Trimerization Catalysts with [NON] and [NSN] Heteroscorpionate Ligands. *Organometallics* **2008**, *27*, 4277–4279. [[CrossRef](#)]
159. Peng, J.; Zhu, M.; Chen, L.; Liu, Z. Unravelling the chain growth mechanism in Cr/NNN-catalysed ethylene oligomerization. *Catal. Sci. Technol.* **2023**, *13*, 6137–6145. [[CrossRef](#)]

160. Ogawa, T.; Lindeperg, F.; Stradiotto, M.; Turculet, L.; Sydora, O.L. Chromium N-phosphinoamidine ethylene tri-/tetramerization catalysts: Designing a step change in 1-octene selectivity. *J. Catal.* **2021**, *394*, 444–450. [\[CrossRef\]](#)
161. Zhou, Y.; Wu, H.; Xu, S.; Zhang, X.; Shi, M.; Zhang, J. Highly active chromium-based selective ethylene tri-/tetramerization catalysts supported by PNPO phosphazane ligands. *Dalton Trans.* **2015**, *44*, 9545–9550. [\[CrossRef\]](#)
162. Manyik, R.M.; Walker, W.E.; Wilson, T.P. A soluble chromium-based catalyst for ethylene trimerization and polymerization. *J. Catal.* **1977**, *47*, 197–209. [\[CrossRef\]](#)
163. Zhang, J.; Alam, F.; Fan, H.; Ma, J.; Jiang, T. Chromium catalysts based on PNP(NR<sub>2</sub>)<sub>2</sub> ligands for selective ethylene oligomerization. *Appl. Organomet. Chem.* **2022**, *36*, e6454. [\[CrossRef\]](#)
164. Kong, W.; Ma, X.; Zuo, J.; Zhao, X.; Zhang, J. Ethylene Tri-/Tetramerization Catalysts Supported by Phenylene-Bridged Mixed Alkyl/Aryl Diphosphine Ligands. *Organometallics* **2023**, *42*, 651–659. [\[CrossRef\]](#)
165. Blann, K.; Bollmann, A.; Dixon, J.T.; Hess, F.M.; Killian, E.; Maumela, H.; Morgan, D.H.; Neveling, A.; Otto, S.; Overett, M.J. Highly selective chromium-based ethylene trimerisation catalysts with bulky diphosphinoamine ligands. *Chem. Commun.* **2005**, 620–621. [\[CrossRef\]](#)
166. Temple, C.; Jabri, A.; Crewdson, P.; Gambarotta, S.; Korobkov, I.; Duchateau, R. The question of the Cr oxidation state in the {Cr(SNS)} catalyst for selective ethylene trimerization: An unanticipated re-oxidation pathway. *Angew. Chem.-Int. Ed.* **2006**, *45*, 7050–7053. [\[CrossRef\]](#)
167. Soheili, M.; Mohamadnia, Z.; Karimi, B. Switching from Ethylene Trimerization to Ethylene Polymerization by Chromium Catalysts Bearing SNS Tridentate Ligands: Process Optimization Using Response Surface Methodology. *Catal. Lett.* **2018**, *148*, 3685–3700. [\[CrossRef\]](#)
168. McGuinness, D.S.; Brown, D.B.; Tooze, R.P.; Hess, F.M.; Dixon, J.T.; Slawin, A.M.Z. Ethylene trimerization with Cr-PNP and Cr-SNS complexes: Effect of ligand structure, metal oxidation state, and role of activator on catalysis. *Organometallics* **2006**, *25*, 3605–3610. [\[CrossRef\]](#)
169. Zhang, J.; Li, A.; Hor, T.S.A. Crystallographic revelation of the role of AIME<sub>3</sub> (in MAO) in Cr [NNN] pyrazolyl catalyzed ethylene trimerization. *Organometallics* **2009**, *28*, 2935–2937. [\[CrossRef\]](#)
170. Alferov, K.A.; Belov, G.P.; Meng, Y. Chromium catalysts for selective ethylene oligomerization to 1-hexene and 1-octene: Recent results. *Appl. Catal. A Gen.* **2017**, *542*, 71–124. [\[CrossRef\]](#)
171. Alam, F.; Zhang, L.; Zhai, Y.; Wang, J.; Tang, H.; Chen, Y.; Jiang, T. In situ formed Cr(III) based silicon-bridged PNS systems for selective ethylene tri-/tetramerization. *J. Catal.* **2019**, *378*, 312–319. [\[CrossRef\]](#)
172. Zhao, X.; Wang, J.; Liu, D.; Kong, W.; Zhang, J. Chromium Ethylene Tri-/Tetramerization Catalysts Supported by Iminophosphine Ligands. *ACS Omega* **2023**, *8*, 34549–34556. [\[CrossRef\]](#)
173. Kuhlmann, S.; Blann, K.; Bollmann, A.; Dixon, J.T.; Killian, E.; Maumela, M.C.; Maumela, H.; Morgan, D.H.; Pr torius, M.; Taccardi, N.; et al. N-substituted diphosphinoamines: Toward rational ligand design for the efficient tetramerization of ethylene. *J. Catal.* **2007**, *245*, 279–284. [\[CrossRef\]](#)
174. McGuinness, D.S.; Wasserscheid, P.; Morgan, D.H.; Dixon, J.T. Ethylene trimerization with mixed-donor ligand (N,P,S) chromium complexes: Effect of ligand structure on activity and selectivity. *Organometallics* **2005**, *24*, 552–556. [\[CrossRef\]](#)
175. Boelter, S.D.; Davies, D.R.; Margl, P.; Milbrandt, K.A.; Mort, D.; Vanchura, B.A.I.; Wilson, D.R.; Wiltzius, M.; Rosen, M.S.; Klosin, J. Phospholane-Based Ligands for Chromium-Catalyzed Ethylene Tri- and Tetramerization. *Organometallics* **2020**, *39*, 976–987. [\[CrossRef\]](#)
176. Alam, F.; Zhang, L.; Wei, W.; Wang, J.; Chen, Y.; Dong, C.; Jiang, T. Catalytic Systems Based on Chromium(III) Silylated-Diphosphinoamines for Selective Ethylene Tri-/Tetramerization. *ACS Catal.* **2018**, *8*, 10836–10845. [\[CrossRef\]](#)
177. Zhang, C.; Song, L.; Wu, H.; Ji, X.; Jiao, J.; Zhang, J. Ethylene tri-/tetramerization catalysts supported by diphosphinothiophene ligands. *Dalton Trans.* **2017**, *46*, 8399–8404. [\[CrossRef\]](#)
178. Radcliffe, J.E.; Batsanov, A.S.; Smith, D.M.; Scott, J.A.; Dyer, P.W.; Hanton, M.J. Phosphanyl Methanimine (PCN) Ligands for the Selective Trimerization/Tetramerization of Ethylene with Chromium. *ACS Catal.* **2015**, *5*, 7095–7098. [\[CrossRef\]](#)
179. Rosenthal, U. PNP-N-H in Comparison to other PNP, PNPN and NP-PN Ligands for the Chromium Catalyzed Selective Ethylene Oligomerization. *ChemCatChem* **2020**, *12*, 41–52. [\[CrossRef\]](#)
180. Lifschitz, A.M.; Hirscher, N.A.; Lee, H.B.; Buss, J.A.; Agapie, T. Ethylene Tetramerization Catalysis: Effects of Aluminum-Induced Isomerization of PNP to PPN Ligands. *Organometallics* **2017**, *36*, 1640–1648. [\[CrossRef\]](#)
181. Zhao, X.; Ma, X.; Kong, W.; Zhang, J. Switchable ethylene tri-/tetramerization with high catalytic performance: Subtle effect presented by P-alkyl substituent of PCCP ligands. *J. Catal.* **2022**, *415*, 95–101. [\[CrossRef\]](#)
182. Choi, E.M.; Park, J.E.; Park, G.S.; Shong, B.; Kang, S.K.; Son, K.s. Selective ethylene oligomerization with in-situ -generated chromium catalysts supported by trifluoromethyl-containing ligands. *J. Polym. Sci. Part A Polym. Chem.* **2018**, *56*, 444–450. [\[CrossRef\]](#)
183. Wang, J.; Gao, R.; Zhang, N.; Tan, X.; Wang, L.; Ma, L.; Shi, W. Novel Dendritic PNP Chromium Complexes: Synthesis, Characterization, and Performance on Ethylene Oligomerization. *Helv. Chim. Acta* **2017**, *100*, e1700162. [\[CrossRef\]](#)
184. Stennett, T.E.; Haddow, M.F.; Wass, D.F. Avoiding MAO: Alternative Activation Methods in Selective Ethylene Oligomerization. *Organometallics* **2012**, *31*, 6960–6965. [\[CrossRef\]](#)
185. Fan, H.; Yang, X.; Ma, J.; Hao, B.; Alam, F.; Huang, X.; Wang, A.; Jiang, T. Computer-assisted design of asymmetric PNP ligands for ethylene tri-/tetramerization: A combined DFT and artificial neural network approach. *J. Catal.* **2023**, *418*, 121–129. [\[CrossRef\]](#)

186. Zhong, X.; Liu, L.; Guo, X.; Sun, L.; Liu, B.; Liu, Z. Cr/PCCP-catalysed selective ethylene oligomerization: Analysis of various conformations and the hemilabile methoxy group. *Catal. Sci. Technol.* **2022**, *12*, 5586–5596. [[CrossRef](#)]
187. Wang, Z.; Liu, L.; Ma, X.; Liu, Y.; Mi, P.; Liu, Z.; Zhang, J. Effect of an additional donor on decene formation in ethylene oligomerization catalyzed by a Cr/PCCP system: A combined experimental and DFT study. *Catal. Sci. Technol.* **2021**, *11*, 4596–4604. [[CrossRef](#)]
188. Yu, Z.-X.; Houk, K.N. Why Trimerization? Computational Elucidation of the Origin of Selective Trimerization of Ethene Catalyzed by  $[TaCl_3(CH_3)_2]$  and An Agostic-Assisted Hydride Transfer Mechanism. *Angew. Chem. Int. Ed.* **2003**, *42*, 808–811. [[CrossRef](#)]
189. Bollmann, A.; Blann, K.; Dixon, J.T.; Hess, F.M.; Killian, E.; Maumela, H.; McGuinness, D.S.; Morgan, D.H.; Neveling, A.; Otto, S.; et al. Ethylene tetramerization: A new route to produce 1-octene in exceptionally high selectivities. *J. Am. Chem. Soc.* **2004**, *126*, 14712–14713. [[CrossRef](#)]
190. Zhang, M.; Wang, K.; Sun, W.-H. Chromium(III) complexes bearing 2-benzazole-1,10-phenanthrolines: Synthesis, molecular structures and ethylene oligomerization and polymerization. *Dalton Trans.* **2009**, 6354–6363. [[CrossRef](#)]
191. Hao, Z.; Xu, B.; Gao, W.; Han, Y.; Zeng, G.; Zhang, J.; Li, G.; Mu, Y. Chromium Complexes with N,N,N-Tridentate Quinolinyl Anilido-Imine Ligand: Synthesis, Characterization, and Catalysis in Ethylene Polymerization. *Organometallics* **2015**, *34*, 2783–2790. [[CrossRef](#)]
192. Luo, W.; Li, A.; Liu, S.; Ye, H.; Li, Z. 2-Benzimidazol-6-pyrazol-pyridine Chromium(III) Trichlorides: Synthesis, Characterization, and Application for Ethylene Oligomerization and Polymerization. *Organometallics* **2016**, *35*, 3045–3050. [[CrossRef](#)]
193. Wang, D.; Liu, S.; Zeng, Y.; Sun, W.-H.; Redshaw, C. 2-Benzimidazolyl-N-phenylquinoline-8-carboxamide Chromium(III) Trichlorides: Synthesis and Application for Ethylene Oligomerization and Polymerization. *Organometallics* **2011**, *30*, 3001–3009. [[CrossRef](#)]
194. Junges, F.; Kuhn, M.C.A.; Dos Santos, A.H.D.P.; Rabello, C.R.K.; Thomas, C.M.; Carpentier, J.-F.; Casagrande, O.L., Jr. Chromium catalysts based on tridentate pyrazolyl ligands for ethylene oligomerization. *Organometallics* **2007**, *26*, 4010–4014. [[CrossRef](#)]
195. Gibson, V.C.; Newton, C.; Redshaw, C.; Solan, G.A.; White, A.J.P.; Williams, D.J. Chromium complexes bearing pyrrolide-imine N,N-chelate ligands: Synthesis, structures and ethylene polymerisation behaviour. *J. Chem. Soc. Dalton Trans.* **2002**, 4017–4023. [[CrossRef](#)]
196. De Oliveira, L.L.; Batista, F.I.; Oliboni, R.S.; Casagrande, A.C.A.; Stieler, R.; Casagrande, O.L. Chromium(III) complexes based on phenoxy-imine ligands with pendant N- and O-donor groups as precatalysts for ethylene oligomerization: Synthesis, characterization, and DFT studies. *J. Organomet. Chem.* **2021**, *936*, 121710. [[CrossRef](#)]
197. Wang, J.; Liu, J.; Chen, L.; Lan, T.; Wang, L. Preparation of chromium catalysts bearing bispyridylamine and its performance in ethylene oligomerization. *Transit. Met. Chem.* **2019**, *44*, 681–688. [[CrossRef](#)]
198. Klemps, C.; Buchard, A.; Houdard, R.; Auffrant, A.; Mézailles, N.; Le Goff, X.F.; Ricard, L.; Saussine, L.; Magna, L.; Le Floch, P. Chromium (III)-bis(iminophosphoranyl)methanido complexes: Synthesis, X-ray crystal structures and catalytic ethylene oligomerization. *N. J. Chem.* **2009**, *33*, 1748–1752. [[CrossRef](#)]
199. Milani, J.L.S.; Biajoli, A.F.P.; Batista, F.I.; Oliboni, R.S.; Casagrande, O.L. Chromium complexes supported by bidentate thioether-imine [N,S] ligands: Synthesis and ethylene oligomerization studies. *N. J. Chem.* **2021**, *45*, 1814–1821. [[CrossRef](#)]
200. Grauke, R.; Schepper, R.; Rabeah, J.; Schoch, R.; Bentrup, U.; Bauer, M.; Brückner, A. Impact of Al Activators on Structure and Catalytic Performance of Cr Catalysts in Homogeneous Ethylene Oligomerization—A Multitechnique in situ/operando Study. *ChemCatChem* **2020**, *12*, 1025–1035. [[CrossRef](#)]
201. Carney, M.J.; Robertson, N.J.; Halfen, J.A.; Zakharov, L.N.; Rheingold, A.L. Octahedral chromium(III) complexes supported by bis(2-pyridylmethyl)amines: Ligand influence on coordination geometry and ethylene polymerization activity. *Organometallics* **2004**, *23*, 6184–6190. [[CrossRef](#)]
202. Lamb, M.J.; Apperley, D.C.; Watson, M.J.; Dyer, P.W. The Role of Catalyst Support, Diluent and Co-Catalyst in Chromium-Mediated Heterogeneous Ethylene Trimerisation. *Top. Catal.* **2018**, *61*, 213–224. [[CrossRef](#)]
203. Fallahi, M.; Ahmadi, E.; Ramazani, A.; Mohamadnia, Z. Trimerization of ethylene catalyzed by Cr-based catalyst immobilized on the supported ionic liquid phase. *J. Organomet. Chem.* **2017**, *848*, 149–158. [[CrossRef](#)]
204. Müller, T.; Dixon, J.T.; Haumann, M.; Wasserscheid, P. Trimerization and tetramerization of ethylene in continuous gas-phase reaction using a Cr-based supported liquid phase catalyst. *React. Chem. Eng.* **2018**, *4*, 131–140. [[CrossRef](#)]
205. Gao, X.; Wang, M.; Chen, Y.; Sun, Y.; Dong, B.; Jiang, T. Biphasic trimerization of ethylene with diphosphinoamine/chromium(III)/methylaluminumoxane immobilized in organochloroaluminate ionic liquid. *React. Kinet. Mech. Catal.* **2014**, *113*, 159–167. [[CrossRef](#)]
206. Goetjen, T.A.; Zhang, X.; Liu, J.; Hupp, J.T.; Farha, O.K. Metal–Organic Framework Supported Single Site Chromium(III) Catalyst for Ethylene Oligomerization at Low Pressure and Temperature. *ACS Sustain. Chem. Eng.* **2019**, *7*, 2553–2557. [[CrossRef](#)]
207. Liu, S.Y.; Zhang, Y.; Han, Y.; Feng, G.L.; Gao, F.; Wang, H.; Qiu, P. Selective Ethylene Oligomerization with Chromium-Based Metal Organic Framework MIL-100 Evacuated under Different Temperatures. *Organometallics* **2017**, *36*, 632–638. [[CrossRef](#)]
208. Agirrezabal-Telleria, I.; Luz, I.; Ortuno, M.A.; Oregui-Bengoechea, M.; Gandarias, I.; Lopez, N.; Lail, M.A.; Soukri, M. Gas reactions under intrapore condensation regime within tailored metal-organic framework catalysts. *Nat. Commun.* **2019**, *10*, 2076. [[CrossRef](#)]
209. LiBretto, N.J.; Xu, Y.; Quigley, A.; Edwards, E.; Nargund, R.; Vega-Vila, J.C.; Caulkins, R.; Saxena, A.; Gounder, R.; Greeley, J.; et al. Olefin oligomerization by main group  $Ga^{3+}$  and  $Zn^{2+}$  single site catalysts on  $SiO_2$ . *Nat. Commun.* **2021**, *12*, 2322. [[CrossRef](#)]

210. Keim, W. Nickel—An element with application in industrial homogeneous catalysis. *Angew. Chem.-Int. Ed. Engl.* **1990**, *29*, 235–244. [[CrossRef](#)]
211. Trofymchuk, O.S.; Gutsulyak, D.V.; Quintero, C.; Parvez, M.; Daniliuc, C.G.; Piers, W.E.; Rojas, R.S. N-Arylciano- $\beta$ -diketiminato Methallyl Nickel Complexes: Synthesis, Adduct Formation, and Reactivity toward Ethylene. *Organometallics* **2013**, *32*, 7323–7333. [[CrossRef](#)]
212. Wang, S.D.; Zhang, W.J.; Du, S.Z.; Asuha, S.; Flisak, Z.; Sun, W.H. Propyl substituted 4-arylimino-1,2,3-trihydroacridylnickel complexes: Their synthesis, characterization and catalytic behavior toward ethylene. *J. Organomet. Chem.* **2015**, *798*, 408–413. [[CrossRef](#)]
213. Fan, H.A.; Zhang, Y.; Alam, F.; Ma, J.; Hao, B.B.; Chen, Y.H.; Wang, Y.T.; Huang, J.M.; Jiang, T. Highly efficient PCCP/Cr(III) ethylene tetramerization catalyst designed using artificial neural network approach. *J. Catal.* **2024**, *429*, 115237. [[CrossRef](#)]
214. Fan, H.N.; Hao, B.B.; Jiang, Y.; Yang, X.D.; Wang, Y.T.; Jiang, T. Selective ethylene tri-/tetramerization chromium catalysts based on binuclear PCCP ligands. *Mol. Catal.* **2023**, *549*, 113545. [[CrossRef](#)]
215. Boelter, S.D.; Davies, D.R.; Milbrandt, K.A.; Wilson, D.R.; Wiltzius, M.; Rosen, M.S.; Klosin, J. Evaluation of Bis(phosphine) Ligands for Ethylene Oligomerization: Discovery of Alkyl Phosphines as Effective Ligands for Ethylene Tri- and Tetramerization. *Organometallics* **2020**, *39*, 967–975. [[CrossRef](#)]
216. Ji, X.Y.; Song, L.B.; Zhang, C.Y.; Jiao, J.J.; Zhang, J. Highly active chromium-based selective ethylene tri-/tetramerization catalysts supported by N,N-diphosphorylamines. *Inorg. Chim. Acta* **2017**, *466*, 117–121. [[CrossRef](#)]

**Disclaimer/Publisher's Note:** The statements, opinions and data contained in all publications are solely those of the individual author(s) and contributor(s) and not of MDPI and/or the editor(s). MDPI and/or the editor(s) disclaim responsibility for any injury to people or property resulting from any ideas, methods, instructions or products referred to in the content.